

Geodesic Distance in Planar Graphs

J. Bouttier¹, P. Di Francesco² and E. Guitter³

Service de Physique Théorique, CEA/DSM/SPhT

Unité de recherche associée au CNRS

CEA/Saclay

91191 Gif sur Yvette Cedex, France

We derive the exact generating function for planar maps (genus zero fatgraphs) with vertices of arbitrary even valence and with two marked points at a fixed geodesic distance. This is done in a purely combinatorial way based on a bijection with decorated trees, leading to a recursion relation on the geodesic distance. The latter is solved exactly in terms of discrete soliton-like expressions, suggesting an underlying integrable structure. We extract from this solution the fractal dimensions at the various (multi)-critical points, as well as the precise scaling forms of the continuum two-point functions and the probability distributions for the geodesic distance in (multi)-critical random surfaces. The two-point functions are shown to obey differential equations involving the residues of the KdV hierarchy.

03/03

¹ bouttier@spht.saclay.cea.fr

² philippe@spht.saclay.cea.fr

³ gutter@spht.saclay.cea.fr

1. Introduction

The study of the statistical properties of random graphs is relevant for many problems in physics, such as two-dimensional quantum gravity or fluid membrane statistics. By random graphs, we here mean graphs *embedded* in a surface of given genus, also known as *fatgraphs* or *maps*. Indeed, these are the natural discretization of fluctuating surfaces, on which matter systems may be defined. Much is known to this day on the enumeration of maps of fixed genus either by combinatorial techniques [1] or by the use of matrix integrals [2-4]. When applied to graphs of large size, these results give rise to various scaling behaviors depending on the critical universality class at hand, described in the continuum by the coupling to 2D quantum gravity of some 2D Conformal Field Theories (CFT) with central charges $c < 1$. In particular, the critical behaviors are characterized by the famous KPZ scaling relations [5]. As an example, the so-called one-matrix model, which enumerates fatgraphs with vertices of arbitrary valence and of any fixed topology, displays a set of multicritical points corresponding to the CFT's with central charges $c(2, 2m + 1)$, $m = 1, 2, 3, \dots$. The first value $m = 1$ corresponds to $c = 0$, i.e. a model of pure 2D quantum gravity without matter, representing the universality class of generic random maps of large size. The higher order multicritical points may be reached by weighting vertices according to their valence, and by suitably fine-tuning the vertex weights.

Most results obtained so far concern *global* properties of the graphs which, in the continuum, can be translated into correlation functions integrated over the positions of their insertion points on the surfaces. Little is known however on more refined properties of random graphs such as the dependence of correlators on the distances between their insertion points. By distance we mean here *geodesic distance* along the graph, namely the length of any shortest path between say two given faces. These refined properties seem to remain beyond the reach of the standard matrix model treatment. Still, some results were obtained in Refs.[6-8], where in particular combinatorial arguments were used to derive the universal scaling two-point function for critical genus zero surfaces with two marked points at a fixed geodesic distance. However, an explicit form for the two-point function was obtained only in the pure gravity case and close to the critical point.

More recently, using a completely different combinatorial approach, the same result was recovered in Ref.[9] in the case of random tetravalent planar maps. This work relies on the existence of a bijection between planar tetravalent maps and rooted trees with vertices labelled by the geodesic distance to the root. The construction however is specific to the tetravalent case, and does not provide a closed form for the discrete solution either.

In this note, we address the general question of the enumeration of planar maps with two marked faces at a fixed geodesic distance. In the case of maps with inner vertices of arbitrary even valence, we derive explicit expressions for the generating function G_n of “two-leg diagrams”, namely planar maps with two distinguished univalent vertices (legs) whose adjacent faces lie at a geodesic distance n of one-another, and with weights g_i per inner $2i$ -valent vertex, $i = 1, 2, 3, \dots$. These results are obtained via the use of a more general bijection between two-leg diagrams and decorated trees first found in Ref.[10] and extended in Ref.[11], which we adapt so as to keep track of the geodesic distance between the two legs. This leads to a simple algebraic recursion relation on n , which allows to derive a closed expression for the solution G_n . We give several explicit expressions depending on the maximum valence of the vertices of the graph. With these solutions in hand, we easily derive the continuum scaling two-point functions corresponding to the various multicritical points. This allows to recover the results of Refs.[7] and [9] in the generic critical case, and also provides the generalization to all higher order multicritical points. We also extract critical exponents such as the fractal dimension in various approaches to the multicritical points, as well as probability distributions for the (rescaled) geodesic distance in multicritical planar maps of fixed but large size.

The paper is organized as follows. In Sect.2 we detail the general correspondence between two-leg diagrams and decorated trees. Sect.3 is devoted to the incorporation of the geodesic distance n between the two legs in this setting and leads to a general recursion relation on n . This recursion relation is solved first in the tetravalent case (Sect.4.1), and exploited to derive a critical fractal dimension $d_F = 4$ (Sect.4.2) and to recover the known continuum two-point function for critical surfaces (Sect.4.3). We also use our explicit solution to derive in Sect.4.4 the probability distribution for rescaled geodesic distances in two-leg diagrams of fixed but large size. The general case of maps with valences up to $2(m + 1)$ is solved in Sect.5, where we discover a remarkable connection with m -soliton solutions of the KP hierarchy. This general solution is applied in Sect.6 to the so-called “hard dimer” model, which displays the first higher order critical point (tricritical point). In Sect.6.1 we detail the solution and display in particular the first few G_n ’s. This leads to the computation in Sect.6.2 of the fractal dimension $d_F = 6$ and the continuum two-point function for tricritical surfaces, corresponding to a generic approach to the tricritical point. We also discuss the case of a non-generic approach along the critical line, which displays another fractal dimension $d_F = 4$ and a different two-point scaling function. We finally obtain in Sect.6.3 the probability distribution for rescaled geodesic distances

in tricritical surfaces of fixed but large size. All these results are extended to the case of the m -th order multicritical point in Sect.7, where we obtain the fractal dimension $d_F = 2(m+1)$ (Sect.7.1), the generic continuum multicritical two-point function (Sect.7.2) and the corresponding probability distribution (Sect.7.3). We gather a few concluding remarks in Sect.8, namely the relation to matrix models (Sect.8.1), the extension to two-point functions of other (less relevant) operators (Sect.8.2), some generalizations to other classes of planar graphs such as constellations (Sect.8.3), as well as a connection to the so-called Integrated SuperBrownian Excursion (ISE) (Sect.8.4). We also gather a few technical details in appendices A and B.

2. Planar maps and decorated trees

There is a general correspondence between planar maps and special classes of decorated trees [10,11]. In this paper, we concentrate on the simpler case of maps with only vertices of *even* valence. In this case, there is a bijection between so-called “two-leg diagrams” and so-called rooted “blossom” trees as defined below. By two-leg diagram, we mean a planar map with two external legs (i.e. two extra univalent vertices) distinguished as in- and out-coming, whereas all inner vertices have even valences. As opposed to the definition used in Ref.[11], we *do not* require that the two external legs lie in the *same* face. By convention, we decide to always represent the diagram in such a way that the in-coming leg is adjacent to the external face in the plane. On the other hand, by rooted blossom trees we mean rooted planar trees with two kinds of endpoints called buds and leaves, with only inner vertices of even valences and such that each inner $2k$ -valent vertex is connected to exactly $k - 1$ buds. It is easily seen that any such tree has exactly *one* more leaf than bud.

The one-to-one correspondence is illustrated in Fig.1. To each two-leg diagram we associate a rooted blossom tree as follows. Starting from the in-coming leg, we iteratively visit all edges of the diagram adjacent to the external face in *counterclockwise* direction. At each step we cut the edge iff the remaining diagram remains connected. The first half of the edge is replaced by a bud, the second one by a leaf. This procedure is repeated with the remaining diagram until a tree is obtained. Finally, the in-coming leg is replaced by a leaf, while the out-coming one is chosen to be the root. It is shown in Refs.[10,11] that the resulting tree is indeed a blossom tree as defined above. This transformation is moreover invertible, by iteratively connecting each bud to the closest available leaf in

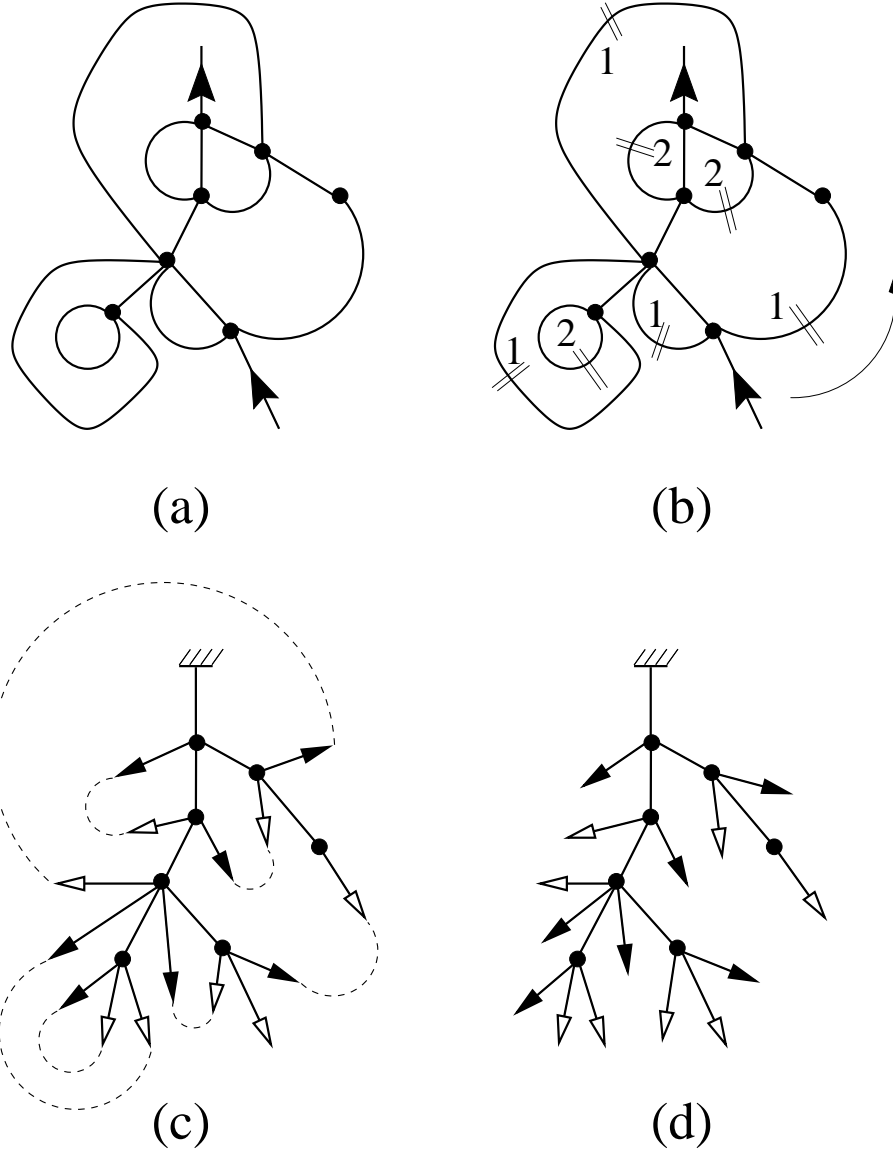


Fig.1: Illustration of the one-to-one correspondence between two-leg diagrams and blossom trees. Starting from a two-leg diagram (a), we apply the iterative cutting procedure explained in the text, which here requires two turns around the graph. The edges cut during the 1st and 2nd turn are displayed in (b) with the corresponding index 1,2. Each cut edge is replaced by a bud-leaf pair (c), while the in-coming leg is replaced by a leaf and the out-coming one by a root, finally leading to a blossom tree (d). Conversely, the matching of buds and leaves of the blossom tree (d) rebuilds the edges of (a).

counterclockwise direction and fusing these bud-leaf pairs into edges. This construction leaves one unmatched leaf, adjacent to the external face, and that we replace by the incoming leg, while the root becomes the out-coming one. Note that in the above fusion

procedure the root may possibly be encompassed by a number of nested edges, in which case it does not lie in the external face. The number of “encompassing” edges will be called the *depth* of the root in the blossom tree.

The generating function R for blossom trees with a weight g_k per $2k$ -valent vertex satisfies

$$R = 1 + \sum_{k \geq 1} g_k \binom{2k-1}{k-1} R^k \quad (2.1)$$

as obtained by inspecting all possible configurations of the vertex attached to the root. The function R is uniquely determined as the formal power series solution of eq.(2.1) in the g_k 's with constant term 1. By the above correspondence, R also coincides with the generating function $\Gamma_{1,1}$ of two-leg diagrams with a weight g_k per inner $2k$ -valent vertex. This is to be contrasted with the generating function Γ_2 for two-leg diagrams with both legs in the external face, or equivalently blossom trees with root at depth 0, which reads [11]

$$\Gamma_2 = R - \sum_{k \geq 2} g_k \binom{2k-1}{k-2} R^{k+1} \quad (2.2)$$

3. Geodesic distance

A nice feature of the above bijection is that it keeps track of the *geodesic distance* between the in- and out-coming legs in the two-leg diagrams, defined as the minimal number of edges crossed by a curve connecting the two legs (for instance, the two legs of the diagram of Fig.1 (a) are at distance 1). Indeed, this distance is nothing but the depth of the root in the corresponding blossom trees. More precisely, it was shown in Refs.[10-12] that all the edges cut in the cutting algorithm belong to minimal paths (i.e. paths crossing a minimal number of edges) going from the external face to all internal ones. In particular, the path from the external face (adjacent to the incoming leg) to that adjacent to the out-coming leg and crossing each encompassing edge exactly once is minimal.

This leads to the refined definition of the generating function G_n for blossom trees with root at depth n , which alternatively generates the two-leg diagrams with geodesic distance n between the legs. In particular, we have $\Gamma_2 = G_0$ and $\Gamma_{1,1} = \sum_{n \geq 0} G_n$. In the following it will prove easier to use the generating function R_n for blossom trees with root at depth *at most* n , such that

$$\begin{aligned} G_n &= R_n - R_{n-1} \\ \Gamma_2 &= R_0 \\ \Gamma_{1,1} &= R = \lim_{n \rightarrow \infty} R_n \end{aligned} \quad (3.1)$$

with the convention that $R_{-1} = 0$.

The first result of this paper is a refined version of eq.(2.1) which keeps track of the depth of the root of the trees.

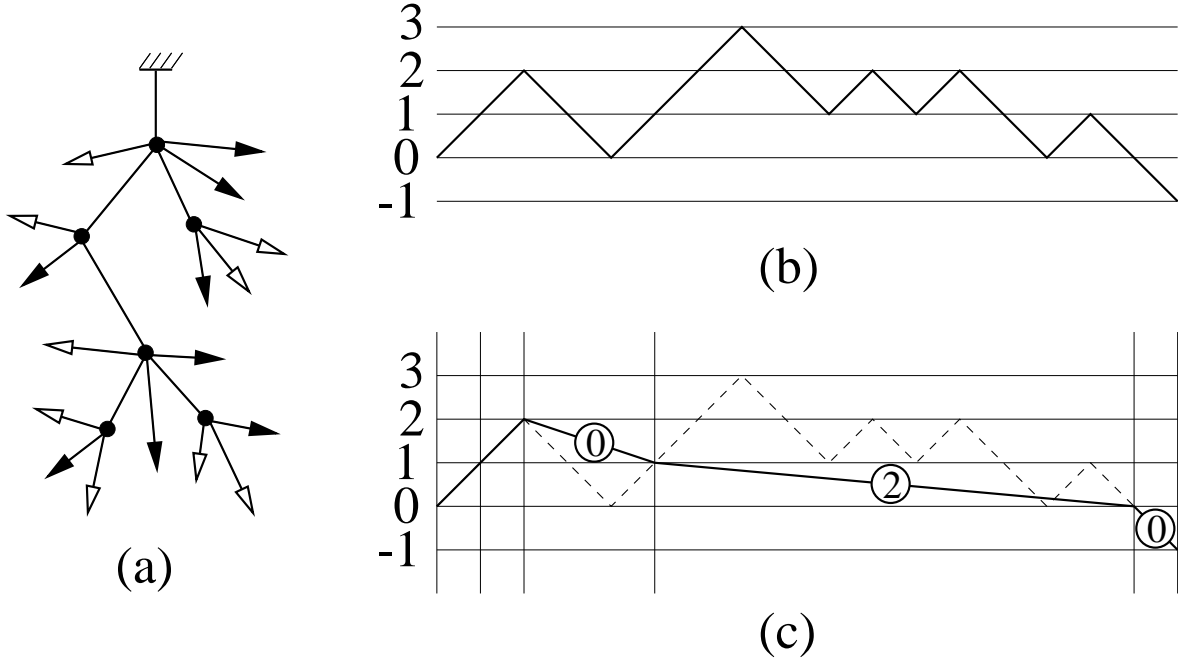


Fig.2: The contour walk (b) associated to a blossom tree (a) obtained by visiting the buds and leaves around the tree in clockwise direction starting from the root. Each bud (resp. leaf) corresponds to a +1 (resp. -1) step. The walk is decomposed in (c) according to the subtrees attached to the root vertex, here two buds and three blossom trees of respective root depths 0, 2, 0, viewed as the maximal relative heights reached by the corresponding portions of walk. Here, the depth of the root is 3, which corresponds to the maximal height attained by the contour walk.

For any blossom tree, let us visit all its buds and leaves successively in clockwise order around the external face starting from the root. This defines the *contour walk* of the tree, namely a walk on the integer line starting from 0 and moving up (height shifted by +1) for each bud encountered and down (height shifted by -1) for each leaf. As leaves are in excess of one on each of these trees, the contour walk stops at height -1. We now easily identify the depth of the root as the maximal height reached by the walk (see Fig.2).

As before, a recursion relation is obtained by inspection of all possible environments of the root in a given blossom tree. In the case of the smallest blossom tree made of a single leaf, the depth of the root is 0, hence this tree contributes 1 to R_n for all $n \geq 0$. In the case of a tree with a $2k$ -valent vertex attached to the root, we have exactly $k - 1$

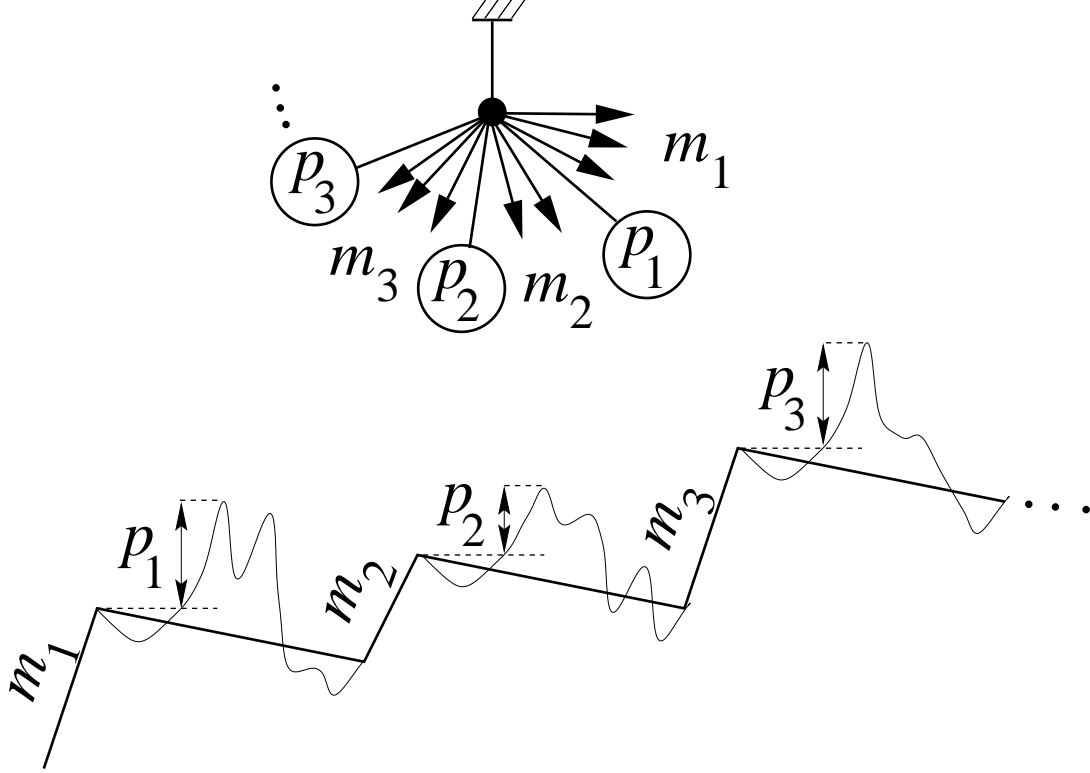


Fig.3: The root vertex environment is characterized by the cyclic sequences of attached buds and blossom subtrees, represented with a circle. The index m_i denotes the number of buds immediately before the i -th blossom subtree, whose root depth is denoted by p_i . The corresponding countour walk is also sketched, and gives a visual representation of eq.(3.2).

buds and k descendent blossom trees attached (see Fig.3). Turning around the vertex in clockwise direction from the root, let m_i denote the (possibly vanishing) number of consecutive buds immediately before the i -th descendent blossom tree, $i = 1, 2, \dots, k$ (with necessarily $\sum m_i \leq k - 1$, $m_i \geq 0$). Let moreover p_i , $i = 1, 2, \dots, k$ denote the depth of the root of the i -th descendent blossom tree, considered as an independent rooted blossom tree. With these definitions, the depth p of the root of the whole tree reads

$$p = \max_{1 \leq i \leq k} \{p_i + m_i + m_{i-1} + \dots + m_1 - (i - 1)\} \quad (3.2)$$

This relation is clear in the countour walk picture, where the walk associated to the whole tree decomposes into $+1$ steps for the buds attached to the vertex, and into subwalks associated with the descendent blossom trees, each contributing by a global -1 height shift. The quantity $p_i + m_i + m_{i-1} + \dots + m_1 - (i - 1)$ is nothing but the maximal height reached within the i -th subwalk, which starts from height $m_i + m_{i-1} + \dots + m_1 - (i - 1)$. From

eq.(3.2), we see that the condition $p \leq n$ is equivalent to $p_i \leq n + i - 1 - m_1 - m_2 - \dots - m_i$ for all $i = 1, 2, \dots, k$, which finally translates into the recursion relation

$$R_n = 1 + \sum_{k \geq 1} g_k \sum_{\substack{m_i \geq 0 \\ m_1 + \dots + m_k \leq k-1}} \prod_{i=1}^k R_{n+i-1-m_1-\dots-m_i} \quad (3.3)$$

with the convention $R_n = 0$ for $n < 0$. This may be viewed as a generalization of eq.(2.1) which is recovered in the limit $n \rightarrow \infty$, where $R_n \rightarrow R$.

The equation (3.3) may be rewritten in an algebraic way by use of a shift operator σ acting on the canonical basis $\{p_n\}_{n \in \mathbb{Z}}$ for sequences as $\sigma p_n = p_{n+1}$, and of its inverse σ^{-1} such that $\sigma^{-1} p_n = p_{n-1}$, namely introducing the operator

$$Q = \sigma + \sigma^{-1} r \quad (3.4)$$

where r acts diagonally as $r p_n = R_n p_n$, eq.(3.3) takes the form

$$Q_{n-1,n} = 1 + \sum_{k \geq 1} g_k (Q^{2k-1})_{n-1,n} \quad (3.5)$$

where $Q_{i,j}$ stand for the matrix elements in the canonical basis $\{p_n\}$. This algebraic formulation (3.5) is very similar to the main recursion relation obtained in the context of one-matrix models with $\mathcal{N} \times \mathcal{N}$ Hermitian matrices and with even potentials of the form $V(M) = \frac{M^2}{2} - \sum_{k \geq 1} g_k \frac{M^{2k}}{2k}$, known to generate fatgraphs with $2k$ -valent vertices weighted by g_k [3]. In this setting, the operator Q represents the multiplication by an eigenvalue λ , acting on polynomials of λ . In the basis made of the monic polynomials $p_n(\lambda)$ orthogonal with respect to the measure $d\lambda e^{-\mathcal{N}V(\lambda)}$ on \mathbb{R} , Q takes the form (3.4) and the recursion relation for the R_n 's takes precisely the form (3.5), except that the first term on the rhs is changed from 1 to n/\mathcal{N} . This coincidence is both remarkable and mysterious as in the matrix model recursion, the R_n 's give access to the generating functions for higher genus graphs, as opposed to the present ones, which only concern planar graphs, but on the other hand allow to explore geodesic distances, a task out of reach in the matrix model.

4. Tetravalent case

4.1. Exact solution

Let us now show how eq.(3.3) may be used to extract exact expressions for the R_n 's. As a first simpler but instructive case, let us restrict our study in this section to the case

of *tetravalent* maps, i.e. two-leg diagrams having only tetravalent inner vertices. Going to generating functions, this amounts to taking $g_k = g\delta_{k,2}$, in which case eq.(2.1) reduces to:

$$R = 1 + 3gR^2 \quad (4.1)$$

with solution

$$R = \frac{1 - \sqrt{1 - 12g}}{6g} \quad (4.2)$$

which displays the well-known critical value $g_c = 1/12$ of g for pure quadrangulations. More generally, the relation (3.3) reduces to:

$$R_n = 1 + gR_n(R_{n-1} + R_n + R_{n+1}) \quad (4.3)$$

Conceptually, this equation, valid for all $n \geq 0$, may be viewed as a recursion of order 2 in n , fully determining all the R_n 's from the initial conditions:

- (i) $R_{-1} = 0$;
- (ii) $R_0 = \Gamma_2$, where Γ_2 is obtained from eqs.(2.2) and (2.1), namely $\Gamma_2 = R - gR^3$ with R as in (4.2).

From the combinatorial origin of the equation, we expect that the non trivial initial condition (ii) may be replaced by the alternative boundary condition at infinity that:

- (ii') $\lim_{n \rightarrow \infty} R_n = R$ with R as in (4.2).

The general solution to eq.(4.3) satisfying (ii') reads:

$$R_n = R \frac{(1 - \lambda x^{n+1})(1 - \lambda x^{n+4})}{(1 - \lambda x^{n+2})(1 - \lambda x^{n+3})} \quad (4.4)$$

where λ is an arbitrary "integration" constant and x is the solution of the characteristic equation:

$$\frac{1 - 4gR}{gR} = x + \frac{1}{x} \quad (4.5)$$

with $|x| < 1$. Note that for $0 \leq g \leq g_c$, the lhs is larger or equal to 2, hence x is real and positive. The condition $0 \leq x < 1$ (which ensures the convergence (ii') of R_n to R) can always be satisfied for $g < g_c$.

That the expression (4.4) solves eq.(4.3) may be checked explicitly. In a more constructive way, this solution is obtained by expanding R_n in the vicinity of R as $R_n = R(1 - \rho_n)$ and first expressing eq.(4.3) at first order in ρ_n with the resulting linearized equation

$$\rho_n^{(1)} = gR(\rho_{n-1}^{(1)} + \rho_n^{(1)} + \rho_{n+1}^{(1)}) + 3gR\rho_n^{(1)} \quad (4.6)$$

The general solution of this linear recursion such that $\lim_{n \rightarrow \infty} \rho_n^{(1)} = 0$ has the form $\rho_n^{(1)} = \alpha_1 x^n$ where x is the solution of the characteristic equation (4.5) with $|x| < 1$. Further expanding R_n , we have

$$\rho_n = \sum_{i \geq 1} \alpha_i (x^n)^i \quad (4.7)$$

Substituting $R_n = R(1 - \rho_n)$ and picking the term of order $k + 1$ in x^n yields the relation

$$\alpha_{k+1} \left(x^{k+1} + \frac{1}{x^{k+1}} - x - \frac{1}{x} \right) = \sum_{j=1}^k \alpha_j \alpha_{k+1-j} \left(x^j + \frac{1}{x^j} + 1 \right) \quad (4.8)$$

solved recursively as

$$\alpha_k = \alpha_1 \left(\frac{\alpha_1 x}{(1-x)(1-x^2)} \right)^{k-1} \frac{1-x^k}{1-x} \quad (4.9)$$

Picking $\alpha_1 = x(1-x)(1-x^2)\lambda$, R_n is easily resummed into (4.4).

Further imposing the initial condition (i) fixes $\lambda = 1$, hence

$$\begin{aligned} R_n &= R \frac{(1-x^{n+1})(1-x^{n+4})}{(1-x^{n+2})(1-x^{n+3})} \\ &= R \frac{U_n(w)U_{n+3}(w)}{U_{n+1}(w)U_{n+2}(w)} \end{aligned} \quad (4.10)$$

where the U_n 's are the Chebyshev polynomials of the first kind, namely obeying $U_{n+1}(w) = wU_n(w) - U_{n-1}(w)$ and $U_0 = 1$, $U_1 = w$, expressed in the variable

$$w = \sqrt{x} + \frac{1}{\sqrt{x}} = \sqrt{\frac{1-2gR}{gR}} \quad (4.11)$$

A first outcome of this solution is that it allows to recover the value of Γ_2 , namely

$$\Gamma_2 = R_0 = R \frac{x + \frac{1}{x}}{1 + x + \frac{1}{x}} = R \frac{1 - 4gR}{1 - 3gR} = R - gR^3 \quad (4.12)$$

as expected, which *a posteriori* shows the equivalence (ii) \leftrightarrow (ii').

As an illustration of the result (4.10), we list below the first few generating functions $G_n(g) = R_n - R_{n-1}$ for two-leg diagrams with legs at a geodesic distance $n = 0, 1, 2, \dots$

$$\begin{aligned} G_0(g) &= \frac{24g - 1 + \sqrt{1-12g}}{9g(1 + \sqrt{1-12g})} = 1 + 2g + 9g^2 + 54g^3 + 378g^4 + 2916g^5 + \dots \\ G_1(g) &= \frac{27g - 2 + (2-15g)\sqrt{1-12g}}{27g(1-8g + \sqrt{1-12g})} = g + 8g^2 + 65g^3 + 554g^4 + 4922g^5 + \dots \\ G_2(g) &= \frac{252g^2 - 6g - 1 + (1+12g)\sqrt{1-12g}}{27(190g^2 - 51g + 3 + (3-33g + 44g^2)\sqrt{1-12g})} \\ &= g^2 + 15g^3 + 179g^4 + 1995g^5 + \dots \end{aligned} \quad (4.13)$$

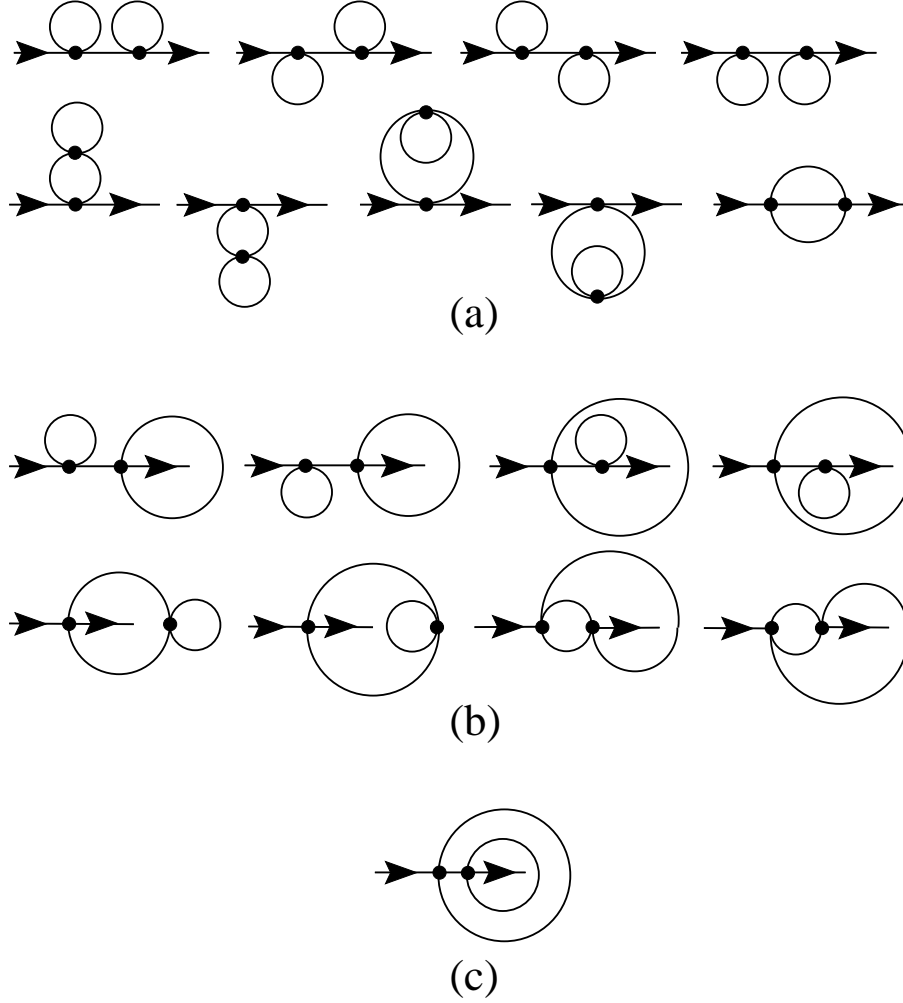


Fig.4: The tetraivalent two-leg diagrams with two inner vertices, classified according to the geodesic distance n between the two legs, namely $n = 0$ (a), $n = 1$ (b) and $n = 2$ (c).

We have represented in Fig.4 all the two-leg diagrams with 2 vertices, among which 9 (resp. 8, 1) have the two legs at geodesic distance 0 (resp. 1, 2), in agreement with the g^2 terms in eq.(4.13).

4.2. Fractal dimension

As a direct application of the solution (4.10), let us evaluate the “fractal dimension” of large tetraivalent planar maps, defined via the number $R_{n,N}$ of two-leg diagrams with distance less or equal to n between the two legs and with N vertices. Indeed, at large N , the limiting ratio

$$B_n \equiv \lim_{N \rightarrow \infty} \frac{R_{n,N}}{R_{0,N}} \quad (4.14)$$

may be taken as a good estimate of the average number of points at a geodesic distance less or equal to n from a given point in random tetravalent maps of infinite size. It is expected to behave like

$$B_n \sim n^{d_F} \quad \text{for large } n \quad (4.15)$$

where d_F is the fractal dimension.

We have

$$R_{n,N} = \oint \frac{dg}{2i\pi g^{N+1}} R_n \quad (4.16)$$

where we must use the expression (4.10) for R_n , in which we substitute expression (4.2) for $R(g)$ and solve eq.(4.5) for x as a function of g . Upon performing the change of variable $g \rightarrow v = gR(g)$, namely $g(v) = v(1 - 3v)$, we arrive at

$$R_{n,N} = \oint \frac{dv(1-6v)}{2i\pi(v(1-3v))^{N+1}} \frac{1}{1-3v} \frac{(1-x(v)^{n+1})(1-x(v)^{n+4})}{(1-x(v)^{n+2})(1-x(v)^{n+3})} \quad (4.17)$$

where we have used $R(g(v)) = 1/(1-3v)$ and the expression $x = x(v) \equiv (1 - 4v - \sqrt{1 - 8v + 12v^2})/(2v)$. The large N behavior is obtained by a saddle-point approximation, with the result

$$R_{n,N} \sim \text{const.} \frac{(12)^N}{N^{\frac{5}{2}}} \frac{(n+1)(n+4)}{(n+2)(n+3)} (140 + 270n + 179n^2 + 50n^3 + 5n^4) \quad (4.18)$$

which finally gives the ratio

$$B_n = \frac{3}{280} \frac{(n+1)(n+4)}{(n+2)(n+3)} (140 + 270n + 179n^2 + 50n^3 + 5n^4) \sim \frac{3}{56} n^4 \quad (4.19)$$

which yields $d_F = 4$, as expected for pure gravity.

4.3. Critical scaling

A continuum limit may be reached by letting g tend to its critical value $g_c = 1/12$, corresponding to $gR \rightarrow 1/6$ and $x \rightarrow 1$. More precisely, we write

$$g = \frac{1}{12}(1 - \epsilon^4) \quad gR = \frac{1}{6}(1 - \epsilon^2) \quad (4.20)$$

from eq.(4.2). In turn, the characteristic equation (4.5) yields

$$x = e^{-a\epsilon} + O(\epsilon^2) \quad a = \sqrt{6} \quad (4.21)$$

As seen from eq.(4.10), a sensible limit is obtained by writing

$$n = \frac{r}{\epsilon} \quad (4.22)$$

and letting $\epsilon \rightarrow 0$. Writing the scaling variable r as $r = n/\xi$, we see that ϵ plays the role of the inverse of the correlation length ξ . As we approach the critical point, we have $\xi = \epsilon^{-1} = ((g_c - g)/g_c)^{-\nu}$ with a critical exponent $\nu = 1/4$, in agreement with $\nu = 1/d_F$, as expected from general principles. Performing this limit explicitly on the solution (4.10) yields an explicit formula for the continuum partition function $\mathcal{F}(r)$ of surfaces with two marked points at a geodesic distance *larger or equal to* r :

$$\mathcal{F}(r) \equiv \lim_{\epsilon \rightarrow 0} \frac{R - R_n}{\epsilon^2 R} = -2 \frac{d^2}{dr^2} \text{Log} \sinh(\sqrt{\frac{3}{2}} r) = \frac{3}{\sinh^2(\sqrt{\frac{3}{2}} r)} \quad (4.23)$$

Upon differentiating with respect to r , we obtain the continuum partition function for surfaces with two marked points at a geodesic distance *equal to* r :

$$\mathcal{G}(r) = -\mathcal{F}'(r) = 3\sqrt{6} \frac{\cosh(\sqrt{\frac{3}{2}} r)}{\sinh^3(\sqrt{\frac{3}{2}} r)} \quad (4.24)$$

in agreement with the form obtained in Ref.[7].

Note that the precise form of the scaling function $\mathcal{F}(r)$ may alternatively be obtained by solving the continuum counterpart of eq.(4.3). Indeed, writing

$$R_n = R(1 - \epsilon^2 \mathcal{F}(n\epsilon)) \quad (4.25)$$

and expanding eq.(4.3) up to order 4 in ϵ , we obtain the following differential equation

$$\mathcal{F}''(r) - 3\mathcal{F}^2(r) - 6\mathcal{F}(r) = 0 \quad (4.26)$$

It is easy to check that $\mathcal{F}(r)$ as given by (4.23) is the unique solution of (4.26) with boundary conditions $\mathcal{F}(r) \rightarrow \infty$ when $r \rightarrow 0$ and $\mathcal{F}(r) \rightarrow 0$ when $r \rightarrow \infty$.

4.4. Continuum probability distribution for geodesic distances

The scaling function $\mathcal{G}(r)$ obtained in the previous subsection is the continuum “two-point function” for surfaces with two marked points at geodesic distance r . It is obtained in a grand-canonical formalism, in which the area of the surfaces (number of vertices in the corresponding maps) is not fixed. In particular, $\mathcal{G}(r)$ cannot be interpreted as

a probability distribution as it is not normalizable. Such a problem does not occur in the *canonical* formalism, i.e. when working with maps of fixed area N . A well defined probability is given by $R_{n,N}/R_{\infty,N}$, where $R_{n,N}$ is the number of two-leg diagrams with N inner vertices and legs distant by at most n , as before, and $R_{\infty,N}$ is the *total* number of two-leg diagrams with N inner vertices. Starting from the expression (4.16) for $R_{n,N}$ and performing again the change of variables $g = v(1 - 3v)$, we get

$$R_{n,N} = \oint \frac{dv(1-6v)}{2i\pi(v(1-3v))^{N+1}} R_n(v) \quad (4.27)$$

where the integral is to be taken on a small contour around the origin. At large N , the integral is dominated by the saddle-point $v = V_c = 1/6$. We therefore perform the change of variables $v = V_c(1 + iu/\sqrt{N})$, with u to be integrated on the real line when $N \rightarrow \infty$. As opposed to the computation of Sect.4.2 where $R_{n,N}$ was estimated for *finite* n and large N , we may obtain a non-trivial distribution by letting $N \rightarrow \infty$ while n scales as $n = \alpha N^{1/4}$, in which case we may use eq.(4.25) with $\epsilon = \sqrt{-iu}/N^{1/4}$, namely

$$\begin{aligned} R_n(v) &= R \left(1 + i \frac{u}{\sqrt{N}} \mathcal{F}(\alpha\sqrt{-iu}) + O\left(\frac{1}{N}\right) \right) \\ &= \frac{V_c}{g_c} \left(1 + \frac{iu}{\sqrt{N}} + O\left(\frac{1}{N}\right) \right) \left(1 + i \frac{u}{\sqrt{N}} \mathcal{F}(\alpha\sqrt{-iu}) + O\left(\frac{1}{N}\right) \right) \\ &= 2 \left(1 + \frac{iu}{\sqrt{N}} \left(1 + \mathcal{F}(\alpha\sqrt{-iu}) \right) \right) + O\left(\frac{1}{N}\right) \end{aligned} \quad (4.28)$$

Substituting this into eq.(4.27), we find

$$\begin{aligned} R_{n,N} &\sim 2 \frac{12^N}{\pi N^{3/2}} \int_{-\infty}^{\infty} du u^2 e^{-u^2} \left(1 + \mathcal{F}(\alpha\sqrt{-iu}) \right) \\ &= 4 \frac{12^N}{\pi N^{3/2}} \int_0^{\infty} du u^2 e^{-u^2} \left(1 + \text{Re} \left(\mathcal{F}(\alpha\sqrt{-iu}) \right) \right) \end{aligned} \quad (4.29)$$

and a similar expression for the limit $R_{\infty,N}$, obtained by taking $\mathcal{F} \rightarrow 0$ in the above. This leads to the probability $\Phi(\alpha)$ for a random two-leg diagram to have legs at a rescaled geodesic distance less than α :

$$\Phi(\alpha) = \frac{2}{\sqrt{\pi}} \int_0^{\infty} du u^2 e^{-u^2} \frac{\cosh(2\alpha\sqrt{3u}) + \cos(2\alpha\sqrt{3u}) + 8 \cosh(\alpha\sqrt{3u}) \cos(\alpha\sqrt{3u}) - 10}{(\cosh(\alpha\sqrt{3u}) - \cos(\alpha\sqrt{3u}))^2} \quad (4.30)$$

Some remarks are in order concerning this explicit form. First we may explicitly expand the probability distribution $\Phi(\alpha)$ as a formal power series of α , with the result

$$\Phi(\alpha) = 6 \sum_{j=1}^{\infty} (-1)^{j+1} \alpha^{4j} 3^{2j} \frac{(2j)!}{j!(4j)!} B_{4j+2} \quad (4.31)$$

where B_j denote the Bernoulli numbers. This series has a radius of convergence zero but provides an asymptotic expansion valid to any finite order. In particular, the leading small α behavior is $\Phi(\alpha) \sim 3\alpha^4/28$, which translates into the equivalent $R_{n,N} \sim (3/28)(n^4/N)R_{\infty,N}$ for finite n and large N , while from eq.(4.19) we have $R_{n,N} \sim (3/56)n^4 R_{0,N}$. These relations are compatible, as we know that $R_{0,N} = 2R_{\infty,N}/(N+2)$ from combinatorial arguments [10].

Secondly, upon differentiating with respect to α , we obtain the probability distribution $\rho(\alpha)$ for two-leg diagrams with legs at rescaled geodesic distance α , with the result:

$$\rho(\alpha) = \frac{4}{\sqrt{\pi}\alpha} \int_0^{\infty} du u^2 (2u^2 - 3) e^{-u^2} \times \frac{\cosh(2\alpha\sqrt{3u}) + \cos(2\alpha\sqrt{3u}) + 8 \cosh(\alpha\sqrt{3u}) \cos(\alpha\sqrt{3u}) - 10}{(\cosh(\alpha\sqrt{3u}) - \cos(\alpha\sqrt{3u}))^2} \quad (4.32)$$

At large α , the function $\rho(\alpha)$ decays as $\exp(-C\alpha^\delta)$, with $C = 3(3/8)^{2/3}$ and with a critical exponent $\delta = 4/3$, in agreement with Fisher's law $\delta = 1/(1-\nu)$, a result already observed in Ref.[7].

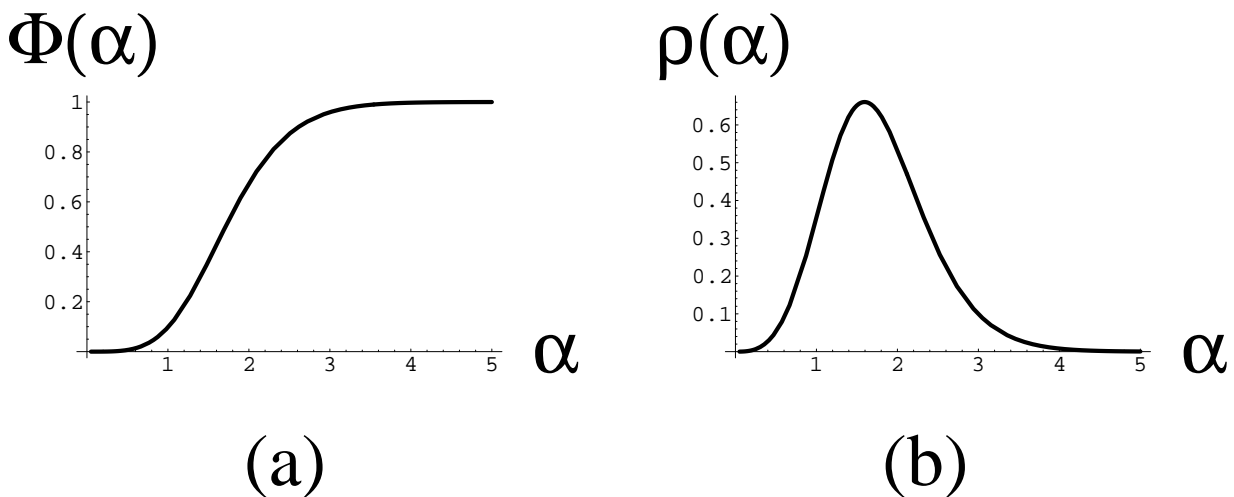


Fig.5: Plots of the probability distributions $\Phi(\alpha)$ (a) and $\rho(\alpha)$ (b) for two-leg diagrams with legs at rescaled geodesic distance at most (a) or equal to (b) α .

The distributions $\Phi(\alpha)$ and $\rho(\alpha)$ are plotted in Fig.5 for illustration.

5. Exact solution in the general case

Let us now turn to the general case of maps with bounded valences, namely with arbitrary even valences $2, 4, 6, \dots$ up to say $2(m+1)$. This corresponds to keeping arbitrary vertex weights g_1, g_2, \dots, g_{m+1} while setting $g_j = 0$ for $j > m+1$. The equation (3.3) becomes a recursion relation of order $2m$ namely expressing R_{n+m} in terms of R_{n+j} , $j = m-1, m-2, \dots, -m$. This equation is valid for all $n \geq 0$, upon taking the initial condition

$$(i) \quad R_{-1} = R_{-2} = \dots = R_{-m} = 0.$$

To completely fix the solution, the condition (i) must be supplemented by

$$(ii) \quad \text{the data of the } m \text{ first terms } R_0, R_1, \dots, R_{m-1}.$$

The explicit combinatorial expression for R_0 is known from the identification with the two-leg function Γ_2 , given by eq.(2.2). As to the other R_j , $j = 1, 2, \dots, m-1$, no direct combinatorial expression is available yet. In view of the previous section, and from the combinatorial interpretation of R_n , we replace the initial data (ii) above with the condition (ii') $\lim_{n \rightarrow \infty} R_n = R$, where R is the solution of eq.(2.1).

As we shall see, this latter condition is indeed sufficient, together with initial condition (i) to completely fix the solution R_n .

To reach this solution, we follow the same strategy as in the tetravalent case of Sect.4. We first obtain constructively the solutions to eq.(3.3) with the only boundary condition (ii'), expressed in terms of m free "integration constants" $\lambda_1, \dots, \lambda_m$. We finally implement the boundary condition (i) to further fix these constants.

Starting with the condition (ii'), let us first expand R_n around its limit as $R_n = R(1 - \rho_n)$ and express eq.(3.3) at first order in ρ_n

$$\begin{aligned} \rho_n^{(1)} &= \sum_{k=0}^m g_{k+1} R^k \sum_{j=-k}^k \left(\sum_{\substack{l=|j| \\ l=j \bmod 2}}^{2k-|j|} \binom{l}{\frac{j+l}{2}} \binom{2k-l}{\frac{j+2k-l}{2}} \right) \rho_{n+j}^{(1)} \\ &= \sum_{k=0}^m g_{k+1} R^k \sum_{j=-k}^k \left(\sum_{l=0}^{k-|j|} \binom{2k+1}{l} \right) \rho_{n+j}^{(1)} \end{aligned} \tag{5.1}$$

The coefficient of $\rho_{n+j}^{(1)}$ in the first line is easily obtained in the contour walk picture as the number of walks from height n to height $n-1$ with $2k+1$ steps and a marked step

down from height $n + j$, itself decomposed into a walk from height n to $n + j$ and say l steps, and a walk from height $n + j - 1$ to $n - 1$ with $2k - l$ steps. Looking for a solution $\rho_{n+j}^{(1)} = \alpha_1 x^n$, we get the characteristic equation

$$\begin{aligned} \chi_m(x) = 0, \quad \chi_m(x) &\equiv 1 - \sum_{k=0}^m g_{k+1} R^k \sum_{l=0}^k \binom{2k+1}{l} \frac{1}{x^{k-l}} \frac{1 - x^{2k+1-2l}}{1-x} \\ &= 1 - \sum_{k=0}^m g_{k+1} R^k \sum_{l=0}^k \binom{2k+1}{l} U_{2k-2l}(w) \end{aligned} \quad (5.2)$$

where the U 's are the Chebyshev polynomials of the first kind, with again $w = \sqrt{x} + 1/\sqrt{x}$. Note that $\chi_m(x)$ is invariant under the interchange $x \leftrightarrow 1/x$, and moreover is a polynomial of degree m in $x + 1/x$. The most general solution $\rho_n^{(1)}$ is a linear combination

$$\rho_n^{(1)} = \sum_{j=1}^m \alpha_j x_j^n \quad (5.3)$$

where x_j , $j = 1, 2, \dots, m$ are the m zeros of χ_m with modulus less than 1. Further expanding ρ_n order by order in the x_j^n , as $\rho_n = \sum_{n_1, \dots, n_m \geq 0} \alpha_{n_1, \dots, n_m} (x_1^n)^{n_1} \dots (x_m^n)^{n_m}$ with $\alpha_{0,0, \dots, 0} = 0$ and $\alpha_{0, \dots, 0, 1, 0, \dots, 0} = \alpha_j$ for the 1 in position j , we get a recursion relation for the coefficients α_{n_1, \dots, n_m} , which determines them all in terms of the initial integration constants $\alpha_1, \dots, \alpha_m$ of (5.3). Upon redefining them like in previous section as $\alpha_i = x_i(1 - x_i)(1 - x_i^2)\lambda_i$, and resumming the expression for R_n , we arrive at

$$\begin{aligned} R_n &= R \frac{u_n^{(m)} u_{n+3}^{(m)}}{u_{n+1}^{(m)} u_{n+2}^{(m)}} \\ u_n^{(m)} &= \sum_{l=0}^m (-1)^l \sum_{1 \leq m_1 < \dots < m_l \leq m} \prod_{i=1}^l \lambda_{m_i} x_{m_i}^{n+m} \prod_{1 \leq i < j \leq l} c_{m_i, m_j} \\ c_{a,b} &\equiv \frac{(x_a - x_b)^2}{(1 - x_a x_b)^2} \end{aligned} \quad (5.4)$$

where, as before, the x_i must be chosen so that $\chi_m(x_i) = 0$, $|x_i| < 1$, $i = 1, 2, \dots, m$. Proving this result is beyond the scope of the present paper. That the form (5.4) actually solves (3.3) with x 's solutions of eq.(5.2) with modulus less than 1 may be explicitly checked for small values of $m = 2, 3, 4$.

A few remarks are in order regarding the particular form (5.4). First the expression (5.4) as a function of R and of the x_i 's is completely independent of the particular values of

the parameters g_k . The link with the specific eq.(3.3) appears only through the expression for R solving (2.1) and the characteristic equation (5.2) satisfied by the x 's. The form of $u_n^{(m)}$ is reminiscent of that of the so-called N-soliton tau-function of the KP hierarchy [13] with the generic form

$$\tau = \sum_{r=0}^N \sum_{i_1 < \dots < i_r} \prod_{\mu=1}^r e^{\eta_{i_\mu}} \left(\prod_{\mu < \nu} c_{i_\mu, i_\nu} \right) \quad (5.5)$$

$$c_{i,j} = \frac{(p_i - p_j)(q_i - q_j)}{(p_i - q_j)(q_i - p_j)}$$

where the η 's contain the times' dependence of the KP hierarchy. We see that, at least from a formal point of view, our solution (5.4) corresponds to taking $N = m$, $e^{\eta_i} = -x_i^{n+m} \lambda_i$, $p_i = x_i$ and $q_i = 1/x_i$. This relation, though suggestive, remains mysterious at present. Secondly, we note that any "N-soliton" solution of the form (5.4) with $m \rightarrow N > m$ reduces to the m -soliton solution when we pick the x 's among the m zeros of χ_m with modulus less than 1. Indeed, for $N > m$, some of the x 's will be equal resulting in the vanishing of the corresponding $c_{i,j}$'s. Analogously, taking an $N < m$ solution is perfectly licit, as it amounts to taking some λ 's to zero, but it corresponds to a less generic solution. In particular, the one-soliton solution (4.4) is solution to all general equations, provided x solves the corresponding characteristic equation. Thirdly, inspired by the determinantal form of various soliton expressions, we find that $u_n^{(m)}$ of eq.(5.4) may be written as the following determinant

$$u_n^{(m)} = \det M_n^{(m)} \quad (5.6)$$

$$[M_n^{(m)}]_{i,j} = \delta_{i,j} - \lambda_i x_i^{n+m} \frac{1 - x_i^2}{1 - x_i x_j} \quad i, j = 1, 2, \dots, m$$

as proved in Appendix A below.

Eq.(5.4) provides the general solution to (3.3) *a priori* valid for any n (not necessarily positive or zero), that satisfies the convergence condition (ii'). Further imposing the initial conditions (i) also implies, by writing (3.3) for $n = -1, -2, \dots, -(m-1)$ that R_{-m-1} and R_{-m-2} diverge and that $R_{-m-3}, R_{-m-4}, \dots, R_{-(2m-1)}$ vanish, which in turn entail that $u_{-1}^{(m)} = 0, u_{-2}^{(m)} = 0, \dots, u_{-(2m-1)}^{(m)} = 0$. These latter conditions entirely fix the values of λ_i to be

$$\lambda_i = \prod_{j \neq i} \frac{1 - x_i x_j}{x_i - x_j} \quad i = 1, 2, \dots, m \quad (5.7)$$

At these values of the λ 's, the solution R_n takes the following particularly simple form:

$$R_n = R \frac{U_n(w_1, \dots, w_m) U_{n+3}(w_1, \dots, w_m)}{U_{n+1}(w_1, \dots, w_m) U_{n+2}(w_1, \dots, w_m)} \quad (5.8)$$

where

$$U_n(w_1, \dots, w_m) \equiv \det [U_{n+2j-2}(w_i)]_{1 \leq i, j \leq m} \quad (5.9)$$

in terms of Chebyshev polynomials of the first kind expressed at values $w_i = \sqrt{x_i} + 1/\sqrt{x_i}$, $i = 1, 2, \dots, m$. Eqs.(5.8)-(5.9) are proved in Appendix B below, by showing that $u_n^{(m)} \propto U_n(w_1, \dots, w_m)$ where the proportionality factors drop out of the ratio giving R_n . The initial conditions $u_{-r}^{(m)} = 0$ for $r = 1, 2, \dots, 2m - 1$ translate for the choice (5.7) of the λ 's into the equivalent conditions that $U_{-r}(w_1, \dots, w_m) = 0$. The latter conditions are clearly satisfied, as direct consequences of the reflection symmetry of the Chebyshev polynomials, namely that $U_{-n-2}(w) = -U_n(w)$ for all n (in particular $U_{-1}(w) = 0$), and therefore, as a determinant, $U_{-r}(w_1, \dots, w_m)$ always has at least two opposite lines (for even r) or a vanishing one (for odd r), provided r stays in the range $1, 2, \dots, 2m - 1$. More precisely, this observation leads to a rank $\text{Int}[(1+r)/2]$ for the matrix with determinant $U_{-r}(w_1, \dots, w_m)$. This gives an *a posteriori* justification of the choice (5.7) for the λ 's.

6. Application: the hard dimer model

6.1. The hard dimer model

As a first application of the exact solution of Sect.5, let us consider the so-called hard dimer model on tetravalent planar maps [14]. In this model, we enumerate tetravalent maps whose edges may be occupied or not by a dimer, with the hardness condition that no two adjacent edges may be simultaneously occupied by dimers. Assigning as usual a weight g per vertex and an activity z per dimer, the problem may be reformulated as that of enumerating maps with both tetra and hexa-valent vertices with a weight $g_2 = g$ per tetravalent vertex and $g_3 = 3zg^2$ per hexavalent one. This is readily seen by shrinking the occupied edges, thus forming hexavalent vertices out of adjacent pairs of tetravalent ones, as shown in Fig.6. Conversely, any given hexavalent vertex may be split into a pair of adjacent tetravalent ones in three different manners, hence the factor of 3. This is a particular case of the general model of previous section with $m = 2$. Note that in the hard dimer language, the notion of geodesic distance must be understood modulo the restriction that the minimal path between the two in- and out-coming legs *must not* cross any edge

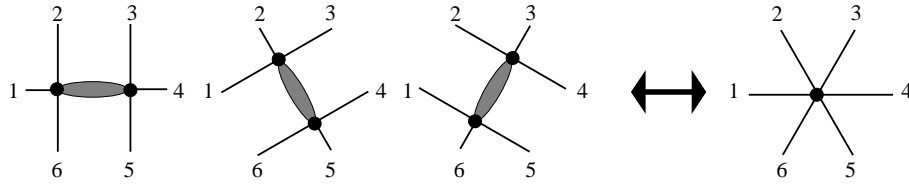
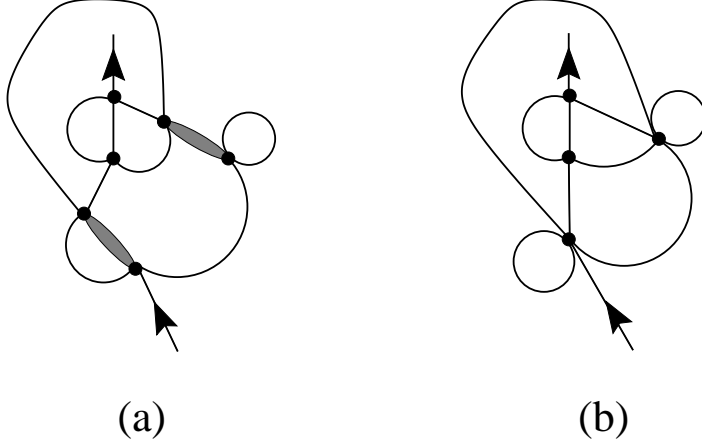


Fig.6: Example (a) of tetraivalent two-leg diagram with hard dimers, represented by thickened edges. The corresponding diagram obtained by shrinking the dimers (b) has both tetraivalent and hexavalent vertices. The correspondence is three-to-one per dimer, as shown.

occupied by a dimer. Indeed, after shrinking occupied edges it would correspond to going through an hexavalent vertex, which is forbidden in the language of graphs with tetra- and hexa-valent vertices.

In the hard dimer case, eq.(2.1) reads

$$R = 1 + 3gR^2 + 30zg^2R^3 \quad (6.1)$$

while the recursion (3.3) reads

$$R_n = 1 + gR_n(R_{n-1} + R_n + R_{n+1}) + 3zg^2R_n(R_{n-2}R_{n-1} + R_{n-1}^2 + R_{n-1}R_{n+1} + R_{n+1}^2 + R_{n+1}R_{n+2} + R_n(2R_{n-1} + R_n + 2R_{n+1})) \quad (6.2)$$

The solution now reads

$$R_n = R \frac{U_n(w_1, w_2)U_{n+3}(w_1, w_2)}{U_{n+1}(w_1, w_2)U_{n+2}(w_1, w_2)} \quad (6.3)$$

where

$$U_n(w_1, w_2) = U_n(w_1)U_{n+2}(w_2) - U_{n+2}(w_1)U_n(w_2) \quad (6.4)$$

and $w_i = \sqrt{x_i} + 1/\sqrt{x_i}$, with x_1, x_2 the solutions with modulus less than one of the characteristic equation

$$\chi_2(x) = 0 \quad \chi_2(x) \equiv 1 - gR \left(x + \frac{1}{x} + 4 \right) - 3zg^2R^2 \left(x^2 + 6x + 16 + \frac{6}{x} + \frac{1}{x^2} \right) \quad (6.5)$$

With this we find the initial terms

$$\begin{aligned} R_0 &= R \frac{1 + (x_1 + \frac{1}{x_1})(x_2 + \frac{1}{x_2})}{1 + (1 + x_1 + \frac{1}{x_1})(1 + x_2 + \frac{1}{x_2})} = R \frac{1 - 4gR - 45zg^2R^2}{1 - 3gR - 30zg^2R^2} \\ R_1 &= R \frac{1 - 7gR + (11 - 78z)g^2R^2 + 234zg^3R^3 + 1215z^2g^4R^4}{(1 - 3gR - 30zg^2R^2)(1 - 4gR - 45zg^2R^2)} \\ R_2 &= \frac{1 - 8gR + (15 - 93z)g^2R^2 + 366zg^3R^3 + 1836z^2g^4R^4}{(1 - 4gR - 45zg^2R^2)(1 - 7gR + (11 - 78z)g^2R^2 + 234zg^3R^3 + 1215z^2g^4R^4)} \end{aligned} \quad (6.6)$$

Note that using eq.(6.1) we may recast $R_0 = R - gR^3(1 + 15zgR)$ which is in agreement with the general formula (2.2) for the two-leg diagram generating function, hence corroborating the relation $R_0 = \Gamma_2$. Finally, we may expand the first few G_i 's as

$$\begin{aligned} G_0(g; z) &= 1 + 2g + 3(3 + 5z)g^2 + 18(3 + 10z)g^3 + 18(21 + 105z + 50z^2)g^4 + \dots \\ G_1(g; z) &= g + 4(2 + 3z)g^2 + (65 + 201z)g^3 + 2(277 + 1305z + 585z^2)g^4 + \dots \\ G_2(g; z) &= (1 + 3z)g^2 + 3(5 + 21z)g^3 + (179 + 1005z + 531z^2)g^4 + \dots \end{aligned} \quad (6.7)$$

As an illustration, we have represented in Fig.7 the two-leg diagrams with two vertices and one hard dimer, corresponding to the terms of order g^2z in eq.(6.7).

6.2. Tricritical point and fractal dimension

The hard dimer model possesses a tricritical point characterized as follows. Introducing the notation $V = gR$, the eq.(6.1) reads

$$g = W(V) \equiv V(1 - 3V - 30zV^2) \quad (6.8)$$

The critical line of the model is characterized by the requirement that $W'(V) = 0$, leading to the parametric curve

$$g = V \left(\frac{2}{3} - V \right) \quad z = \frac{1 - 6V}{90V^2} \quad (6.9)$$

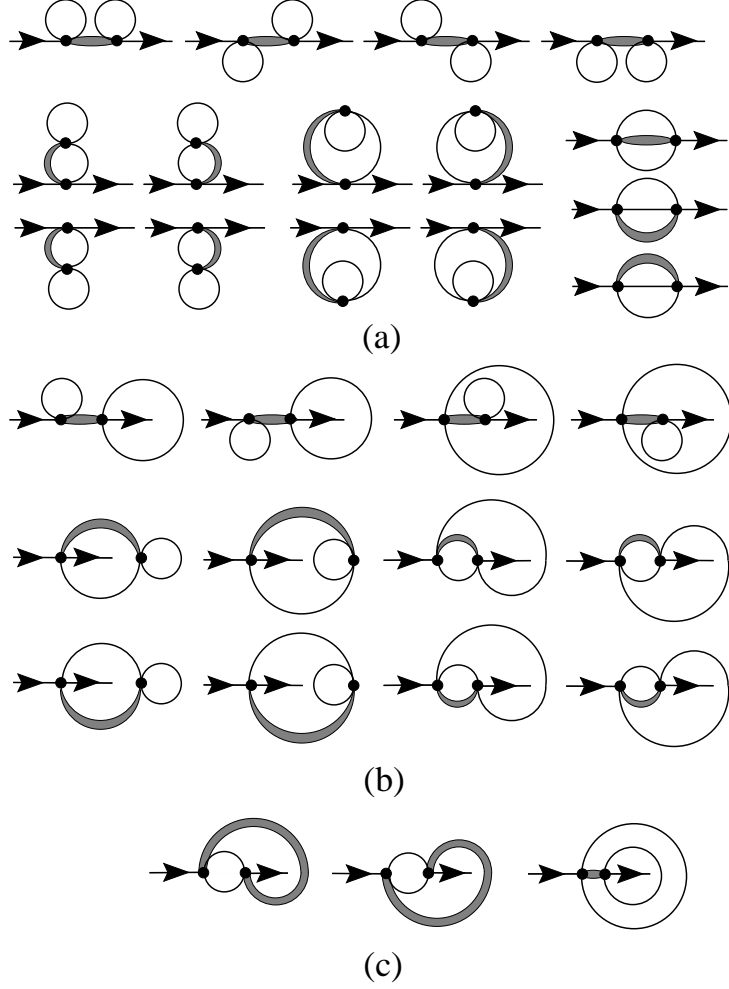


Fig.7: The tetraivalent two-leg diagrams with two inner vertices and one dimer are represented according to the distance n between the two legs, respectively $n = 0$ (a), $n = 1$ (b) and $n = 2$ (c). Note that the two first diagrams of (c) have $n = 2$ as we forbid crossing the dimer.

for $0 < V \leq 1/3$. The curve ends at a higher order tricritical point where, in addition we have $W''(V) = 0$, which fixes the critical values

$$V_c = \frac{1}{3} \quad g_c = \frac{1}{9} \quad z_c = -\frac{1}{10} \quad R_c = 3 \quad (6.10)$$

We may approach this point by first setting $z = z_c = -1/10$ and letting g approach $g_c = 1/9$, in which case eq.(6.8) simplifies into

$$g = g_c \left(1 - \left(\frac{V_c - V}{V_c} \right)^3 \right) \quad (6.11)$$

We therefore set

$$g = g_c(1 - \epsilon^6) \quad V = V_c(1 - \epsilon^2) \quad (6.12)$$

and let $\epsilon \rightarrow 0$. At $z = z_c$, the characteristic equation (6.5) takes a particularly simple form when expressed in the variable $y = x + 1/x - 2$, namely

$$\chi_2(x) = 0 = \frac{3}{10}(Vy)^2 - (1 - 3V)Vy + (1 - 3V)^2 \quad (6.13)$$

We see that at the tricritical point $V = V_c = 1/3$, $y = 0$ is a double root of eq.(6.13), hence $x = 1$ is a quadruple root of the characteristic equation. Moreover, eq.(6.13) amounts to the vanishing of a polynomial of degree 2 in the reduced variable $u = yV/(V_c - V)$, namely $P_2(u) = u^2/30 - u/3 + 1 = 0$ with the two roots $u_{\pm} = 5 \pm i\sqrt{5}$. When approaching the tricritical point via (6.12), we therefore have the solutions

$$y_{\pm} = u_{\pm} \frac{\epsilon^2}{1 - \epsilon^2} \quad (6.14)$$

which imply the following leading behavior for the two x 's with modulus less than 1 solving the characteristic equation:

$$x_{1,2} = x_{\pm} = e^{-\epsilon a_{\pm}} + O(\epsilon^2) \quad a_{\pm} = \sqrt{5 \pm i\sqrt{5}} \quad (6.15)$$

where the square roots are taken with positive real parts. As before, a sensible scaling limit is obtained by writing $n = r/\epsilon$ in eq.(6.3). This amounts to introducing a correlation length $\xi = \epsilon^{-1} = ((g_c - g)/g_c)^{-1/6}$, which leads to a critical exponent $\nu = 1/6$. We may still interpret the quantity $d_F = 1/\nu = 6$ as a tricritical fractal dimension as follows. Like in Sect.4.2, we consider the limiting ratio B_n of (4.14) where $R_{n,N}$ now denotes the partition function for two-leg diagrams with N vertices, distance at most n between the two legs and with hard particles with fugacity $z = z_c$. A straightforward though tedious calculation yields

$$\begin{aligned} B_n &= \frac{1}{16632} \frac{(n+1)(n+6)}{(n+3)(n+4)} \times \\ &\times (33264 + 74088n + 63014n^2 + 26985n^3 + 6215n^4 + 735n^5 + 35n^6) \\ &\sim \frac{5}{2376} n^6 \end{aligned} \quad (6.16)$$

in which we read off $d_F = 6$.

Further, expanding eq.(6.3) at order 2 in ϵ , we obtain the *tricritical scaling function* $\mathcal{F}(r)$ counting surfaces with two marked points at a geodesic distance larger or equal to r :

$$\begin{aligned} \mathcal{F}(r) &\equiv \lim_{\epsilon \rightarrow 0} \frac{R - R_n}{\epsilon^2 R} = -2 \frac{d^2}{dr^2} \text{Log } \mathcal{W} \left(\sinh \left(a_+ \frac{r}{2} \right), \sinh \left(a_- \frac{r}{2} \right) \right) \\ &= - \frac{(a_+^2 - a_-^2) (a_+^2 \sinh^2 (a_- \frac{r}{2}) - a_-^2 \sinh^2 (a_+ \frac{r}{2}))}{2 (a_- \cosh (a_- \frac{r}{2}) \sinh (a_+ \frac{r}{2}) - a_+ \cosh (a_+ \frac{r}{2}) \sinh (a_- \frac{r}{2}))^2} \end{aligned} \quad (6.17)$$

where $\mathcal{W}(f_1, f_2)$ stands for the Wronskian determinant $f_1 f_2' - f_2 f_1'$, and a_{\pm} as in eq.(6.15). As before, the scaling function $\mathcal{G}(r)$ counting surfaces with two marked points at geodesic distance r is obtained by differentiating $-\mathcal{F}(r)$.

So far we have considered a particular approach to the tricritical point, namely with a fixed $z = z_c$. Let us now show that the *same* exponent ν is obtained for any other generic approach to the tricritical point and that moreover the *same* scaling function is obtained, up to a multiplicative redefinition of r . Indeed, expanding the relation $g = W(V)$ around the critical values as $g = g_c + \delta g$, $V = V_c + \delta V$, $z = z_c + \delta z$, we obtain at leading order:

$$\delta g + \frac{10}{9}\delta z = 3(\delta V)^3 \quad (6.18)$$

Taking a generic approach $\delta g = -g_c \alpha \epsilon^6$, $\delta z = -z_c \beta \epsilon^6$, we arrive at $\delta V = -V_c(\alpha - \beta)^{\frac{1}{3}} \epsilon^2$. Accordingly, the characteristic equation (6.5) reads

$$\chi_2(x) = 0 = 3(\delta V)^2 P\left(-\frac{yV_c}{\delta V}\right) + O(\epsilon^6) \quad (6.19)$$

which yields the same solution y_{\pm} as in eq.(6.14) up to a multiplicative factor of $(\alpha - \beta)^{\frac{1}{3}}$, which in turn leads to the same scaling function (6.17) up to a redefinition $r \rightarrow r/(\alpha - \beta)^{\frac{1}{6}}$.

One notable exception is when $\alpha = \beta$, or more precisely when $z_c \delta g = g_c \delta z$ in which case the lhs of (6.18) vanishes at leading order, and we must also consider higher terms in the expansion, namely of the form $\delta z \delta V$. Such a situation occurs in particular if we approach the tricritical point *along the critical line* (6.9). In that case, we have $\delta g = -(\delta V)^2$. Now the appropriate scaling is $\delta g = -g_c \epsilon^4$, and $\delta V = -V_c \epsilon^2$. The expansion of the characteristic equation now leads to another polynomial equation of the form $Q_2(-yV_c/\delta V) = 0$, where $Q_2(u) = u^2/30 - u/3$. This gives the solutions $x_1 = 1$ and $x_2 = e^{-a\epsilon}$, with now $a = \sqrt{10}$. The appropriate scaling of the distance therefore still reads $n = r/\epsilon$, and we have an exponent $\nu = 1/4$ from the behavior of the correlation length $\xi = \epsilon^{-1} = ((g_c - g)/g_c)^{-1/4}$. This particular approach leads to a different scaling function \mathcal{F}_c which can be obtained from the form (6.17) by letting $a_+ \rightarrow 0$ and $a_- = a = \sqrt{10}$, namely

$$\mathcal{F}_c(r) = -2 \frac{d^2}{dr^2} \text{Log}(\sqrt{\frac{5}{2}} r \cosh(\sqrt{\frac{5}{2}} r) - \sinh(\sqrt{\frac{5}{2}} r)) \quad (6.20)$$

To conclude this section, we note that the generic tricritical scaling function $\mathcal{F}(r)$ of eq.(6.17) may be alternatively obtained by deriving the continuum counterpart of eq.(6.2) yielding the following differential equation for $\mathcal{F}(r)$

$$\mathcal{F}^{(4)}(r) - 10\mathcal{F}(r)\mathcal{F}''(r) - 10\mathcal{F}''(r) - 5(\mathcal{F}'(r))^2 + 10(\mathcal{F}(r))^3 + 30(\mathcal{F}(r))^2 + 30\mathcal{F}(r) = 0 \quad (6.21)$$

The scaling function $\mathcal{F}(r)$ of eq.(6.17) is the unique solution to eq.(6.21) such that $\lim_{r \rightarrow 0} r^2 \mathcal{F}(r) = 6$ while $\lim_{r \rightarrow \infty} \mathcal{F}(r) = 0$. The condition at $r \rightarrow 0$ may be seen by writing $\mathcal{F}(r) = -2d^2/dr^2 \text{Log} \mathcal{U}(r)$, where $\mathcal{U}(r)$ is the continuum limit of u_n and imposing the continuum counterpart of the discrete conditions $u_{-1} = u_{-2} = u_{-3} = 0$, namely that $\mathcal{U}(0) = \mathcal{U}'(0) = \mathcal{U}''(0) = 0$, hence $\mathcal{U}(r) \propto r^3$, and $\mathcal{F}(r) \sim 6/r^2$. In the same spirit, the scaling function \mathcal{F}_c of eq.(6.20) corresponding to a non-generic approach of the tricritical point along the critical line is the unique solution with the same boundary conditions as just mentioned of the truncated differential equation

$$\mathcal{F}_c^{(4)}(r) - 10\mathcal{F}_c(r)\mathcal{F}_c''(r) - 10\mathcal{F}_c'(r) - 5(\mathcal{F}_c'(r))^2 + 10(\mathcal{F}_c(r))^3 + 30(\mathcal{F}_c(r))^2 = 0 \quad (6.22)$$

6.3. Continuum probability distribution for geodesic distances

As in Sect.4.4, we may translate the above result into an explicit expression for the probability distribution for geodesic distances in tricritical surfaces with hard dimers. Again, we must compute the ratio $R_{n,N}/R_{\infty,N}$, where $R_{n,N}$ now denotes the generating function for two-leg diagrams with hard dimers at $z = z_c = -1/10$, with N inner vertices and legs distant by at most n . Starting from the contour integral (4.16) applied to the hard dimer problem, we perform the change of variables $g = W(v)$, with W as in (6.8), with the result

$$R_{n,N} = \oint \frac{dv W'(v)}{2i\pi W(v)^{N+1}} R_n(v) \quad (6.23)$$

At large N , this integral is dominated by the saddle-point $v = V_c = 1/3$. We now perform the change of variables $v = V_c(1 - e^{-i\pi \text{sgn}(u)/3} |u|/N^{1/3})$ where u is to be integrated on the real line when $N \rightarrow \infty$. This prescription is obtained by deforming the initial contour of integration around the origin of the v -plane so as to encompass only the image of the pole at $v = 0$. A suitable limit is obtained by further setting $n = \alpha N^{1/6}$, and using

$$\begin{aligned} R_n(v) &= R \left(1 - e^{-i\frac{\pi}{3}} \frac{u}{N^{\frac{1}{3}}} \mathcal{F}(\alpha e^{-i\frac{\pi}{6}} \sqrt{u}) + O\left(\frac{1}{N^{\frac{2}{3}}}\right) \right) \\ &= \frac{V_c}{g_c} \left(1 - e^{-i\frac{\pi}{3}} \frac{u}{N^{\frac{1}{3}}} (1 + \mathcal{F}(\alpha e^{-i\frac{\pi}{6}} \sqrt{u})) + O\left(\frac{1}{N^{\frac{2}{3}}}\right) \right) \end{aligned} \quad (6.24)$$

for $u > 0$ and \mathcal{F} as in eq.(6.17) and the corresponding counterpart for $u < 0$. We finally get

$$R_{n,N} \sim \frac{9^{N+1}}{\pi N^{\frac{4}{3}}} \int_0^\infty du u^3 e^{-u^3} \text{Re} \left(e^{-i\frac{\pi}{6}} (1 + \mathcal{F}(\alpha e^{i\frac{\pi}{6}} \sqrt{u})) \right) \quad (6.25)$$

This leads to the probability for tricritical two-leg diagrams to have a rescaled geodesic distance less than α :

$$\Phi(\alpha) = 6 \frac{\sqrt{3}}{\Gamma(\frac{1}{3})} \int_0^\infty du u^3 e^{-u^3} \operatorname{Re} \left(e^{-i\frac{\pi}{6}} (1 + \mathcal{F}(\alpha e^{i\frac{\pi}{6}} \sqrt{u})) \right) \quad (6.26)$$

and by differentiating with respect to α , to the probability distribution $\rho(\alpha)$ for distances equal to α . Note finally that for small α , we have $\Phi(\alpha) \sim 5\alpha^6/1188$, in agreement with eq.(6.16), while the large α behavior obeys Fisher's law with a decay of the form $\exp(-C\alpha^{6/5})$.

7. General multicritical points: fractal dimensions and scaling functions

7.1. Fractal dimensions

In this section we consider the case of arbitrary m , in which case we may reach an m -th order multicritical point. For simplicity, we set $g_1 = 0$ and we introduce the following notations

$$g_2 = g \quad g_k = g^{k-1} z_k \quad (\text{with } z_2 = 1) \quad V = gR \quad (7.1)$$

$$W(V) = V - \sum_{k=2}^{m+1} z_k \binom{2k-1}{k-1} V^k$$

in terms of which eq.(2.1) reads simply $W(V) = g$. The m -th order multicritical point is obtained by setting $W' = W'' = \dots = W^{(m)} = 0$ which implies

$$z_k^{(c)} = (-1)^k \frac{\frac{1}{m+1} \binom{m+1}{k}}{\binom{2k-1}{k-1}} \left(\frac{6}{m} \right)^{k-1} \quad (7.2)$$

With these, eq.(2.1) simply reads

$$g = W(V) = \frac{V_c^{m+1} - (V_c - V)^{m+1}}{(m+1)V_c^m} \quad V_c = \frac{m}{6} \quad (7.3)$$

while $g_c = W(V_c) = m/(6(m+1))$. For simplicity, we decide to approach the m -th order multicritical point by first setting all the z_k 's to their critical values $z_k^{(c)}$ of eq.(7.2), and then letting g approach g_c . As already shown in the previous section, this approach is sufficient to capture the generic multicritical behavior. As readily seen from eq.(7.3), we must set

$$g = g_c(1 - \epsilon^{2m+2}) \quad V = V_c(1 - \epsilon^2) \quad (7.4)$$

The characteristic equation (5.2) takes a particularly simple form when expressed in the variable $y = x + 1/x - 2$, namely

$$\chi_m(x) = 0 = \sum_{l=0}^m \frac{l!}{(2l+1)!} (Vy)^l \frac{d^{l+1}W(V)}{dV^{l+1}} \quad (7.5)$$

This is a consequence of the following identity for Chebyshev polynomials

$$\sum_{l=0}^k \binom{2k+1}{l} U_{2k-2l}(w) = \frac{(2k+1)!}{k!} \sum_{l=0}^k \frac{l!}{(2l+1)!} \frac{y^l}{(k-l)!} \quad (7.6)$$

where as before $w = \sqrt{x} + 1/\sqrt{x}$. This identity is proved by showing that both sides satisfy the same recursion relation $\beta_{k+1} - a^2\beta_k = \binom{2k+2}{k+1}$, and have the same initial term $\beta_0 = 1$. Eq.(7.5) follows by substituting the identity (7.6) into eq.(5.2). With the value (7.3) of $W(V)$, the characteristic equation becomes

$$\begin{aligned} \chi_m(x) = 0 &= \left(\frac{V_c - V}{V_c}\right)^m P_m\left(\frac{yV}{V_c - V}\right) \\ P_m(u) &= \sum_{l=0}^m (-u)^l \frac{l!}{(2l+1)!} \frac{m!}{(m-l)!} \end{aligned} \quad (7.7)$$

Approaching the multicritical point as in eq.(7.4), we get the solutions

$$y_i = u_i \frac{\epsilon^2}{1 - \epsilon^2} \quad (7.8)$$

where the u_i , $i = 1, 2, \dots, m$ are the distinct roots of P_m . In turn, this yields the x_i 's with modulus less than one

$$x_i = e^{-\epsilon a_i} + O(\epsilon^2) \quad a_i = \sqrt{u_i} \quad (7.9)$$

where the square roots are taken with positive real parts. Again, to get a sensible limit, we must write $n = r/\epsilon$ in eq.(5.8), which displays again a correlation length $\xi = \epsilon^{-1} = ((g_c - g)/g_c)^{-\nu}$, with $\nu = 1/(2m + 2)$. This leads to a generalized multicritical fractal dimension $d_F = 2(m + 2)$.

7.2. Scaling functions

The expansion of eq.(5.8) at order 2 in ϵ gives the general multicritical scaling function

$$\mathcal{F}(r) = -2 \frac{d^2}{dr^2} \text{Log } \mathcal{W} \left(\sinh \left(a_1 \frac{r}{2} \right), \sinh \left(a_2 \frac{r}{2} \right), \dots, \sinh \left(a_m \frac{r}{2} \right) \right) \quad (7.10)$$

where $\mathcal{W}(f_1, f_2, \dots, f_m)$ is the Wronskian determinant $\det [f_i^{(j-1)}]_{1 \leq i, j \leq m}$. This scaling function may alternatively be obtained as the unique solution such that $\lim_{r \rightarrow 0} r^2 \mathcal{F}(r) = 2(2m - 1)$ and $\lim_{r \rightarrow \infty} \mathcal{F}(r) = 0$ of the differential equation

$$\mathcal{R}_{m+1}[1 + \mathcal{F}] = \mathcal{R}_{m+1}[1] \quad (7.11)$$

where $\mathcal{R}_p[\mathbf{u}]$ are the residues of the KdV hierarchy [15], defined recursively by $\mathcal{R}'_{p+1} = \mathcal{R}'''_p/4 - \mathbf{u}\mathcal{R}'_p - \mathbf{u}'\mathcal{R}_p/2$, $\mathcal{R}_0 = 1/2$.

To show eq.(7.11), let us recall that our recursion relation (3.3) coincides with that of the one-matrix model with even potential, up to a change $1 \leftrightarrow n/\mathcal{N}$. More precisely, writing formally eq.(3.3) as $\Psi_n(\{R_j\}; \{g_k\}) = 1$, the corresponding equation in the matrix model reads $\Psi_n(\{R_j\}; \{g_k\}) = n/\mathcal{N}$. Approaching the m -th order critical point with the g_k 's given by eqs.(7.1) and (7.2), and making the scaling ansatz $g = g_c(1 - \epsilon^{2m+2})$, $R_n = R_c(1 - \epsilon^2 \mathbf{u}(n\epsilon))$, the functional Ψ_n may be expanded at small ϵ as

$$\Psi_n(\{R_j\}; \{g_k\}) = 1 + \epsilon^{2m+2}(1 - \mathcal{S}_{m+1}[\mathbf{u}]) + O(\epsilon^{2m+4}) \quad (7.12)$$

where $\mathcal{S}_{m+1}[\mathbf{u}]$ is a functional of \mathbf{u} to be identified. In the context of the matrix model's double-scaling limit, we write $\Psi_n(\{R_j\}; \{g_k\}) = n/\mathcal{N} = 1 + \epsilon^{2m+2}(1 - t)$, where t is the renormalized cosmological constant, which leads to the equation $\mathcal{S}_{m+1}[\mathbf{u}] = t$, where \mathbf{u} is interpreted as the renormalized string susceptibility. From this, we identify $\mathcal{S}_{m+1} \propto \mathcal{R}_{m+1}$, as is well known from random matrix theory [3]. Going back to our problem, the scaling ansatz (4.25) with $R = R_c(1 - \epsilon^2)$ corresponds to having $\mathbf{u} = 1 + \mathcal{F}$ and the equation $\Psi_n(\{R_j\}; \{g_k\}) = 1$ now yields $\mathcal{S}_{m+1}[1 + \mathcal{F}] = 1$. Eq.(7.11) follows by proportionality as we know from eq.(2.1) that $\mathcal{F} = 0$ must be solution.

As an independent check, we may derive a characteristic equation $\pi_m(a^2) = 0$ by linearizing the continuum equation (7.11) and looking for solutions of the form $\mathcal{F}(r) = e^{-ar}$. Using the explicit value $\mathcal{R}_p[1] = (-1)^p \binom{2p}{p} / 2^{2p+1}$, and the recursion relation for the KdV residues, we find the recursion relation $\pi_p(a^2) = (a^2 - 4)\pi_{p-1}(a^2)/4 - (-1)^p \binom{2p}{p} / 2^{2p+2}$, with the initial value $\pi_0 = -1/4$. Solving this recursion explicitly, we simply find that $\pi_m(a^2) = (2m + 1)(-1)^{m-1} \binom{2m}{m} / 2^{2m+2} P_m(a^2)$, with P_m as in eq.(7.7), hence the characteristic equation coincides with $\chi_m(x) = 0$ for $x + 1/x - 2 = \epsilon^2 a^2$.

Two final remarks are in order. First, the scaling function (7.10) is the generic scaling function for the m -th order multicritical point. It may also be obtained by starting with a problem involving vertices up to valences $2m' + 2$, $m' > m$, and approaching any

point of the m -th order critical manifold of dimension $m' - m$, for which the characteristic equation has $x = 1$ as a $2m$ -times degenerate zero. Conversely, we may approach the m -th order multicritical point by first going to an m' -th order multicritical manifold with $m' < m$ (which amounts to having $x = 1$ as a $2m'$ -times degenerate zero of the characteristic equation), and then approaching the m -th order multicritical point along this manifold. The corresponding scaling function is different from the generic one for the m -th order multicritical point and may be obtained as a limit of the form (7.10) in which say $a_1, \dots, a_{m'} \rightarrow 0$ while $a_{m'+1}, \dots, a_m$ tend to the specific values coming from the restriction of the characteristic equation to the m' -critical manifold.

7.3. Probability distribution for geodesic distances

As in Sects.4.4 and 6.3, we may derive expressions for the probability distribution of geodesic distances in multicritical surfaces. Again, we compute the ratio $R_{n,N}/R_{\infty,N}$, where $R_{n,N}$ denotes the generating function for two-leg diagrams at $z_k = z_k^{(c)}$ as given by eq.(7.2), with N inner vertices and legs at distance at most n . In the the contour integral (4.16) for the present multicritical problem, we perform the change of variables $g = W(v)$, with W as in eq.(7.1), to get, as before

$$R_{n,N} = \oint \frac{dv W'(v)}{2i\pi W(v)^{N+1}} R_n(v) \quad (7.13)$$

At large N , the integral is dominated by the saddle-point $v = V_c = m/6$ and we perform the change of variables $v = V_c(1 - e^{-i\frac{\pi \operatorname{sgn}(u)}{m+1}} |u|/N^{\frac{1}{m+1}})$ where u is to be integrated on the real line when $N \rightarrow \infty$. We obtain a suitable limit by further setting $n = \alpha N^{\frac{1}{2(m+1)}}$, and using

$$\begin{aligned} R_n(v) &= R \left(1 - e^{-i\frac{\pi}{m+1}} \frac{u}{N^{\frac{1}{m+1}}} \mathcal{F}(\alpha e^{-i\frac{\pi}{2(m+1)}} \sqrt{u}) + O\left(\frac{1}{N^{\frac{2}{m+1}}}\right) \right) \\ &= \frac{V_c}{g_c} \left(1 - e^{-i\frac{\pi}{m+1}} \frac{u}{N^{\frac{1}{m+1}}} \left(1 + \mathcal{F}(\alpha e^{-i\frac{\pi}{2(m+1)}} \sqrt{u}) \right) + O\left(\frac{1}{N^{\frac{2}{m+1}}}\right) \right) \end{aligned} \quad (7.14)$$

for $u > 0$ with \mathcal{F} as in eq.(7.10) and the corresponding counterpart for $u < 0$. We finally get

$$R_{n,N} \sim \frac{\left(6\frac{m+1}{m}\right)^N (m+1)^2}{\pi N^{\frac{m+2}{m+1}}} \int_0^\infty du u^{m+1} e^{-u^{m+1}} \operatorname{Re} \left(e^{-i\frac{\pi(m-1)}{2(m+1)}} \left(1 + \mathcal{F}(\alpha e^{i\frac{\pi}{2(m+1)}} \sqrt{u}) \right) \right) \quad (7.15)$$

This gives the probability distribution for rescaled geodesic distances at most α

$$\Phi(\alpha) = \frac{(m+1)^2}{\cos\left(\frac{\pi(m-1)}{2(m+1)}\right)\Gamma\left(\frac{1}{m+1}\right)} \int_0^\infty du u^{m+1} e^{-u^{m+1}} \operatorname{Re}\left(e^{-i\frac{\pi(m-1)}{2(m+1)}} (1 + \mathcal{F}(\alpha e^{i\frac{\pi}{2(m+1)}} \sqrt{u}))\right) \quad (7.16)$$

and that for rescaled geodesic distances equal to α by differentiation. As expected, we have $\Phi(\alpha) \propto \alpha^{2(m+1)}$ at small α while $\rho(\alpha)$ decays for large α as $\exp(-C\alpha^{2(m+1)/(2m+1)})$.

8. Discussion and conclusion

In this paper, we have found explicit expressions for partition functions of planar maps with arbitrary even valences and with two marked points at a specified geodesic distance. From these we have extracted various scaling functions and critical exponents corresponding to various approaches to the different critical and multicritical points. We also obtained various probability distributions for distances in maps of fixed but large number of vertices. These results rely on a purely combinatorial technique based on bijections with trees.

8.1. Relation to matrix models and integrability

The results obtained here cannot apparently be reached by the more standard matrix integral approach, which naturally deals with the genus of the graphs rather than with geodesic distances. However, we observe strong analogies between the two problems, as apparent from the structure of our main recursion relation. Even more strikingly, in the continuum limit of the m -critical model, we found a differential equation of the form $\mathcal{R}_{m+1}[\mathbf{u}] = \mathcal{R}_{m+1}[1]$ with $\mathbf{u} = 1 + \mathcal{F}$, to be compared with the generalized KdV equation $\mathcal{R}_{m+1}[\mathbf{u}] = \text{const.}t$ for the all-genus string susceptibility $\mathbf{u}(t)$ where t plays the role of a renormalized cosmological constant in the double-scaling limit [3]. This also amounts to having replaced the usual string equation $[P, Q] = 1$, $Q = d^2 - \mathbf{u}$, $d = d/dt$, and P a differential operator of degree $2m + 1$, by simply $[P, Q] = 0$. This modification is what makes the problem exactly solvable both in the discrete and continuum versions. In particular, we note the appearance of soliton-like expressions for our solutions, which are the sign of an underlying integrable structure.

We expect that this scheme also applies to the general case of a $c(p, q)$ CFT coupled to 2D quantum gravity, namely that the fundamental two-point scaling functions of the geodesic distance are still determined by differential equations of the form $[P, Q] = 0$, where P and Q are differential operators of respective degrees p and q .

8.2. Other two-point functions

The continuum m -multicritical two-point function that we have derived was obtained as the scaling limit of the exact discrete solution. We expect on general grounds that it corresponds to the two-point correlation of the *most relevant* operator ϕ_1 in the corresponding $c(2, 2m+1)$ conformal field theory coupled to 2D quantum gravity. It is clear that many more quantities may be derived from the general solution (5.4). In the language of quantum gravity, this includes in particular correlations of the form $\langle \phi_1(0)\phi_j(r) \rangle$ involving less relevant operators ϕ_j , $j = 2, 3, \dots, m$ as functions of the geodesic distance r . In the language of this paper, natural discrete candidates for such correlators are the generating functions $G_n^{(k)}$ for two-leg diagrams with legs distant by n and such that the outgoing leg is attached to a $2k$ -valent vertex. In this paper we have considered $G_n = \delta_{n,0} + \sum G_n^{(k)}$, a particular linear combination of the $G_n^{(k)}$. In the continuum limit, this combination has a non-vanishing overlap with the most relevant operator ϕ_1 of the theory, hence we may interpret our result as computing $\langle \phi_1(0)\phi_1(r) \rangle \propto \mathcal{G}(r)$. We expect that by considering other fine-tuned linear combinations of the $G_n^{(k)}$, we will obtain higher order terms in ϵ , a term of order ϵ^{2j+1} corresponding to a two-point function $\langle \phi_1(0)\phi_j(r) \rangle$. Indeed, the above linear combinations amount to having inserted some operator ϕ_j at the vertex adjacent to the outgoing leg, while the other leg remains untouched, and therefore still carries ϕ_1 . To compute these two-point functions, we observe that $R_n^{(k)} \equiv \sum_{j=0}^n G_j^{(k)} = g_k(Q^{2k-1})_{n-1,n}$, with notations as in eqs.(3.4)-(3.5). These are the same polynomials of the R_j 's as those appearing in the recursion relation for the one-matrix model, and we may therefore apply the known results on the double-scaling limit in relation with KdV flows to identify

$$\langle \phi_1(0)\phi_j(r) \rangle \propto -\frac{d}{dr} \mathcal{R}_j[1 + \mathcal{F}] \quad (8.1)$$

for $j = 1, 2, \dots, m$, with \mathcal{F} solving eq.(7.11).

These correlators also allow for an explicit exploration of the general problem of fractal dimensions, a subtle question already addressed in Refs.[8, 16].

8.3. Generalizations

We may adapt the techniques of this paper so as to address similar questions in more involved graph enumeration problems. Indeed, the case of planar maps with vertices of even valence that we considered here is a particular case of a more general class of planar maps called p -constellations. These are bipartite planar maps with say black and white

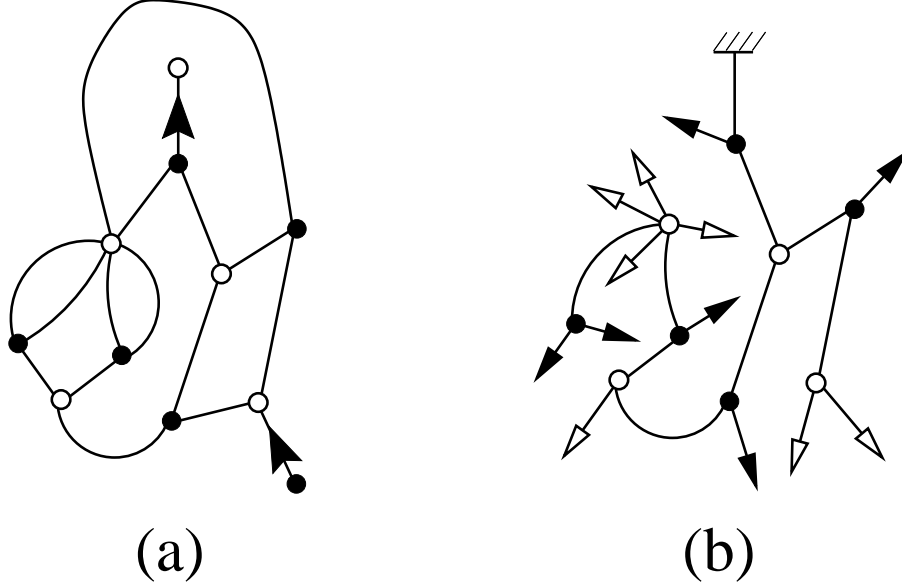


Fig.8: Example (a) of a two-leg 3-constellation with geodesic distance 1, and (b) the corresponding blossom tree (see Ref.[12] for precise definitions and characterizations).

vertices, such that all black vertices are p -valent, while the white ones have valences kp , $k = 1, 2, 3, \dots$. For $p = 2$, the black (two-valent) vertices may be wiped out while the white ones have arbitrary even valences, which is the case studied in this paper. For general $p \geq 3$, we may still consider two-leg diagrams with a univalent black vertex (in-coming leg) and a univalent white one (out-coming leg), not necessarily adjacent to the same face (see Fig.8 for an illustration). The geodesic distance between the legs is the minimal length of paths connecting them, with the constraint that one may only cross edges with the white vertex on the right and therefore the black vertex on the left, when going from the face adjacent to the in-coming leg to that adjacent to the out-coming one. These two-leg diagrams are in one-to-one correspondence with suitable bipartite blossom trees as shown in Ref.[12]. Using this equivalence, and limiting ourselves to white vertex valences up to $(m+1)p$ for some fixed m we have shown that the generating function R_n for two-leg diagrams with legs distant by at most n satisfies a polynomial recursion relation, which allows to determine them exactly. Remarkably, we find that the generic form for R_n is again very similar to that of (5.4), except for a simple shift in the indices of $u_n^{(N)}$, namely

$$R_n = R \frac{u_n^{(N)} u_{n+p+1}^{(N)}}{u_{n+1}^{(N)} u_{n+p}^{(N)}} \quad (8.2)$$

where $R = \lim_{n \rightarrow \infty} R_n$ is a solution of a polynomial equation of degree $(m+1)(p-1)$, $u_n^{(N)}$ is a N -soliton solution to KP of the form (5.5) with $N = (m+1)(p-1) - 1$, $e^{\eta_i} = -x_i^{n+N} \lambda_i$, x_i being the solutions with modulus less than 1 of the characteristic equation associated to the recursion relation (and of degree N in $x + 1/x$), and finally $p_i = x_i + x_i^2 + \dots + x_i^{p-1}$, while $q_i = 1/x_i + 1/x_i^2 + \dots + 1/x_i^{p-1}$. Again, the integration constants λ_i are determined by the initial conditions $u_{-i} = 0$, $i = 1, 2, \dots, (2N - 1)$, which in turn fully specifies the solution R_n . Apart from these complications, the strategy of the present paper may be applied to these more involved cases of p -constellations. In particular, we have checked that we recover the expected generating function $\Gamma_2 = R_0$ previously obtained in Refs.[17-19]. However, we do not expect any new critical behavior or scaling functions other than that already obtained in this paper for $p = 2$.

More promising, the same techniques can be applied to models of graphs with matter degrees of freedom such as the Ising model, whose study is under way [20], and where new scaling functions appear.

8.4. Connection to ISE

Let us finally discuss the relation between the present work and the other combinatorial approach of Ref.[9] for the tetravalent case. In this reference, a different bijection between tetravalent rooted maps and labeled trees is used, where the labels precisely encode the geodesic distance from the root. Representing both the underlying tree and its labels by two discrete 1D random walks, the problem translates into a discrete version of the so-called Brownian snake, which makes the connection between geodesic distances on tetravalent planar maps and random variables of the Integrated SuperBrownian Excursion (ISE). In particular, the continuum distribution $\Phi(\alpha)$ for the simple critical case $m = 1$ coincides with the distribution for the maximum of the ISE, whose suitably defined Laplace transform was obtained in Ref.[21] and coincides with \mathcal{F} . Beyond this $m = 1$ case, it would be interesting to understand in ISE terms the counterpart of our multicritical results for arbitrary m . In particular, eq.(7.16) may be inverted as

$$\mathcal{F}(\alpha) = \frac{1}{(m+1)\Gamma\left(\frac{m}{m+1}\right)} \int_0^\infty \frac{du}{u^{\frac{m+2}{m+1}}} e^{-u} \left(1 - \Phi\left(\frac{\alpha}{u^{\frac{1}{2(m+1)}}}\right) \right) \quad (8.3)$$

which displays the suitably generalized Laplace transform to be used in this case. In the ISE language, this suggests to consider excursions with “duration” u distributed according to a suitably generalized Ito law $P(u) \propto 1/u^{\frac{m+2}{m+1}}$. An example of the discrete version of

such “multicritical excursions” was considered in the context of (1+1)-D Lorentzian gravity in Ref.[22] in the form of walks with steps of heights $1, 2, \dots, m$ with respective weights z_1, \dots, z_m which must be fine-tuned to some multicritical values. Understanding such a connection would provide a direct link between the so-called Lorentzian and Euclidean two-dimensional quantum gravities.

Acknowledgments

We thank F. David, J.-F. Delmas and G. Schaeffer for useful discussions partly while attending the semester “Geometry and statistics of random growth” held at the Institut Henri Poincaré, Paris, January-March 2003. We also thank D. Bernard, R. Conte and M. Musette for help with references on solitons.

Appendix A. Proof of the determinant form (5.6) for $u_n^{(m)}$ of eq.(5.4).

Eq.(5.6) is proved by expanding the determinant as

$$\begin{aligned}
\det M_n^{(m)} &= \sum_{\sigma \in S_m} \text{sgn}(\sigma) \prod_{i=1}^m \left(\delta_{i, \sigma(i)} - \lambda_i x_i^{n+m} \frac{1 - x_i^2}{1 - x_i x_{\sigma(i)}} \right) \\
&= \sum_{\sigma \in S_m} \text{sgn}(\sigma) \sum_{l=0}^m \sum_{1 \leq i_1 < \dots < i_l \leq m} \prod_{j \notin \{i_1, \dots, i_l\}} \delta_{j, \sigma(j)} \prod_{i \in \{i_1, \dots, i_l\}} \left(-\lambda_i x_i^{n+m} \frac{1 - x_i^2}{1 - x_i x_{\sigma(i)}} \right) \\
&= \sum_{l=0}^m (-1)^l \sum_{1 \leq i_1 < \dots < i_l \leq m} \left(\prod_{r=1}^l \lambda_{i_r} x_{i_r}^{n+m} \right) \det \left[\frac{1 - x_{i_s}^2}{1 - x_{i_s} x_{i_t}} \right]_{1 \leq s, t \leq l}
\end{aligned} \tag{A.1}$$

The identification with the form (5.4) for $u_n^{(m)}$ is completed by computing the determinant in the last line of (A.1) as

$$\det \left[\frac{1 - y_s^2}{1 - y_s y_t} \right]_{1 \leq s, t \leq l} = \prod_{1 \leq s < t \leq l} \left(\frac{y_s - y_t}{1 - y_s y_t} \right)^2 \tag{A.2}$$

where $y_s \equiv x_{i_s}$, obtained by direct application of the Cauchy determinant formula

$$\det \left[\frac{1}{y_s + z_t} \right]_{1 \leq s, t \leq l} = \frac{\prod_{1 \leq s < t \leq l} (y_s - y_t)(z_s - z_t)}{\prod_{1 \leq s, t \leq l} (y_s + z_t)} \tag{A.3}$$

upon taking $z_s = -1/y_s$.

Appendix B. Proof of the determinant form (5.8)-(5.9).

Let us start from the determinant formula (5.6) in which we substitute the values (5.7) of the λ_i :

$$u_n^{(m)} = \det M_n^{(m)}$$

$$[M_n^{(m)}]_{i,j} = \delta_{i,j} - x_i^{n+m} \frac{\prod_{l \neq j} 1 - x_i x_l}{\prod_{l \neq i} x_i - x_l} \quad i, j = 1, 2, \dots, m \quad (\text{B.1})$$

We now multiply $M_n^{(m)}$ to the right by the matrix $P^{(m)}$ with entries

$$[P^{(m)}]_{i,j} = \frac{x_i^{m-j}}{\prod_{l \neq i} x_i - x_l} \quad (\text{B.2})$$

This gives the general term

$$[M_n^{(m)} P^{(m)}]_{i,j} = \frac{x_i^{m-j}}{\prod_{l \neq i} x_i - x_l} \left(1 - x_i^{n+j} \sum_{k=1}^m x_k^{1-j} \prod_{l \neq k} \frac{1 - x_i x_l}{1 - \frac{x_l}{x_k}} \right) \quad (\text{B.3})$$

Defining

$$\varphi_j(x) = \sum_{k=1}^m x_k^{1-j} \prod_{l \neq k} \frac{1 - x x_l}{1 - \frac{x_l}{x_k}} \quad (\text{B.4})$$

we see that $\varphi_j(x)$ is the Lagrange interpolation polynomial of degree less or equal to $m-1$, that takes the values $\varphi_j(1/x_k) = x_k^{1-j}$ at the m distinct points $x = 1/x_k$, for $k = 1, 2, \dots, m$. We conclude that $\varphi_j(x) = x^{j-1}$ for $j = 1, 2, \dots, m$. This allows to finally rewrite (B.3) as

$$[M_n^{(m)} P^{(m)}]_{i,j} = \frac{x_i^{m+\frac{n-1}{2}}}{\prod_{l \neq i} x_i - x_l} \left(\frac{1}{x_i^{\frac{n-1}{2}+j}} - x_i^{\frac{n-1}{2}+j} \right)$$

$$= \frac{x_i^{m+\frac{n-1}{2}}}{\prod_{l \neq i} x_i - x_l} \left(\frac{1}{\sqrt{x_i}} - \sqrt{x_i} \right) U_{n+2j-2}(w_i) \quad (\text{B.5})$$

with $w_i = \sqrt{x_i} + 1/\sqrt{x_i}$ as before. Taking the determinant, we arrive at

$$u_n^{(m)} = \frac{1}{\det P^{(m)}} \prod_{i=1}^m \left(\frac{x_i^{m+\frac{n-1}{2}} \left(\frac{1}{\sqrt{x_i}} - \sqrt{x_i} \right)}{\prod_{l \neq i} x_i - x_l} \right) \times \det [U_{n+2j-2}(w_i)]_{1 \leq i, j \leq m} \quad (\text{B.6})$$

which immediately leads to eqs.(5.8)-(5.9), by noting that all the prefactors drop out of the ratio.

References

- [1] W. Tutte, *A Census of planar triangulations* Canad. Jour. of Math. **14** (1962) 21-38; *A Census of Hamiltonian polygons* Canad. Jour. of Math. **14** (1962) 402-417; *A Census of slicings* Canad. Jour. of Math. **14** (1962) 708-722; *A Census of Planar Maps*, Canad. Jour. of Math. **15** (1963) 249-271.
- [2] E. Brézin, C. Itzykson, G. Parisi and J.-B. Zuber, *Planar Diagrams*, Comm. Math. Phys. **59** (1978) 35-51.
- [3] P. Di Francesco, P. Ginsparg and J. Zinn-Justin, *2D Gravity and Random Matrices*, Physics Reports **254** (1995) 1-131.
- [4] B. Eynard, *Random Matrices*, Saclay Lecture Notes (2000), available at http://www-spht.cea.fr/lectures_notes.shtml
- [5] V.G. Knizhnik, A.M. Polyakov and A.B. Zamolodchikov, *Fractal Structure of 2D Quantum Gravity*, Mod. Phys. Lett. **A3** (1988) 819-826; F. David, *Conformal Field Theories Coupled to 2D Gravity in the Conformal Gauge*, Mod. Phys. Lett. **A3** (1988) 1651-1656; J. Distler and H. Kawai, *Conformal Field Theory and 2D Quantum Gravity*, Nucl. Phys. **B321** (1989) 509-527.
- [6] H. Kawai, N. Kawamoto, T. Mogami and Y. Watabiki, *Transfer Matrix Formalism for Two-Dimensional Quantum Gravity and Fractal Structures of Space-time*, Phys. Lett. B **306** (1993) 19-26.
- [7] J. Ambjørn and Y. Watabiki, *Scaling in quantum gravity*, Nucl.Phys. **B445** (1995) 129-144.
- [8] J. Ambjørn, J. Jurkiewicz and Y. Watabiki, *On the fractal structure of two-dimensional quantum gravity*, Nucl.Phys. **B454** (1995) 313-342.
- [9] P. Chassaing and G. Schaeffer, *Random Planar Lattices and Integrated SuperBrownian Excursion*, preprint (2002), to appear in Probability Theory and Related Fields, math.CO/0205226.
- [10] G. Schaeffer, *Bijective census and random generation of Eulerian planar maps*, Electronic Journal of Combinatorics, vol. **4** (1997) R20; see also G. Schaeffer, *Conjugaison d'arbres et cartes combinatoires aléatoires* PhD Thesis, Université Bordeaux I (1998).
- [11] J. Bouttier, P. Di Francesco and E. Guitter, *Census of planar maps: from the one-matrix model solution to a combinatorial proof*, Nucl. Phys. **B645**[PM] (2002) 477-499.
- [12] M. Bousquet-Mélou and G. Schaeffer, *Enumeration of planar constellations*, Adv. in Applied Math., **24** (2000) 337-368.
- [13] M. Jimbo and T. Miwa, *Solitons and infinite dimensional Lie algebras*, Publ. RIMS, Kyoto Univ. **19** No. 3 (1983) 943-1001, eq.(2.12).
- [14] M. Staudacher, *The Yang-Lee Edge Singularity on a Dynamical Planar Random Surface*, Nucl. Phys. **B336** (1990) 349-362.

- [15] I. Gelfand and L. Dikii, *Fractional powers of operators and Hamiltonian systems*, Funct. Anal. Appl. **10:4** (1976) 13.
- [16] N. Kawamoto and K. Yotsuji, *Numerical study for the c -dependence of fractal dimension in two-dimensional quantum gravity*, Nucl.Phys. **B644** (2002) 533-567.
- [17] J. Bouttier, P. Di Francesco and E. Guitter, *Counting colored Random Triangulations*, Nucl.Phys. **B641** (2002) 519-532.
- [18] M. Bousquet-Mélou and G. Schaeffer, *The degree distribution in bipartite planar maps: application to the Ising model*, preprint math.CO/0211070.
- [19] J. Bouttier, P. Di Francesco and E. Guitter, *Combinatorics of hard particles on planar maps* preprint (2002) to appear in Nucl. Phys. **B**, cond-mat/0211168.
- [20] J. Bouttier, P. Di Francesco and E. Guitter, work in progress.
- [21] J.-F. Delmas *Computation of moments for the length of the one dimensional ISE support*, preprint (2002), available at <http://cermics.enpc.fr/~delmas/>.
- [22] P. Di Francesco and E. Guitter, *Critical and multicritical semi-random $(1 + d)$ -dimensional lattices and hard objects in d dimensions*, J. Phys. A Math. Gen, **35** (2002) 897-927.